Multi-tiered actions of *Legionella* effectors to modulate host Rab10 dynamics

Tomoko Kubori[a*], Kohei Arasaki[b], Tomoe Kitao[a], and Hiroki Nagai[a,c*]

[a]Department of Microbiology, Graduate School of Medicine, Gifu University, Gifu, Gifu 501-1194, Japan

[b]School of Life Sciences, Tokyo University of Pharmacy and Life Sciences, Hachioji, Tokyo 192-0392, Japan

[c]Center for One Medicine Innovative Translational Research, Gifu University Institute for Advanced Study, Gifu, Gifu 501-1194, Japan

*Correspondence: kubori.tomoko.j0@f.gifu-u.ac.jp (T. Ku.) and nagai.hiroki.d3@f.gifu-u.ac.jp (H. N.)

Abstract

Rab GTPases are representative targets of manipulation by intracellular bacterial pathogens for hijacking membrane trafficking. *Legionella pneumophila* recruits many Rab GTPases to its vacuole and exploits their activities. Here, we found that infection-associated regulation of Rab10 dynamics involves ubiquitin signaling cascades mediated by the SidE and SidC families of *Legionella* ubiquitin ligases. Phosphoribosyl-ubiquitination of Rab10 catalyzed by the SidE ligases is crucial for its recruitment to the bacterial vacuole. SdcB, the previously uncharacterized SidC family effector, resides on the vacuole and contributes to retention of Rab10 at the late stages of infection. We further identified MavC as a negative regulator of SdcB. By the transglutaminase activity, MavC crosslinks ubiquitin to SdcB and suppresses its function, resulting in elimination of Rab10 from the vacuole. These results demonstrate that the orchestrated actions of many *L. pneumophila* effectors fine-tune the dynamics of Rab10 during infection.

Introduction

Legionella pneumophila utilizes a large arsenal of effector proteins which are delivered via its Dot/Icm type IV secretion system (T4SS) to modulate host cellular systems (Hubber and Roy, 2010; Kubori and Nagai, 2016). The functions of the effector proteins are crucial for establishing a replicative niche where *L. pneumophila* can survive and avoid host defense mechanisms in the cell (Isberg et al., 2009; Qiu and Luo, 2017). Many effector proteins are known to modulate the function of host Rab GTPases that regulates cellular membrane transport (Neunuebel and Machner, 2012; Sherwood and Roy, 2013; Spanò and Galán, 2018). Among them, effector manipulation of Rab1, a critical regulator of membrane trafficking between ER and the Golgi complex, has been extensively analyzed in *L. pneumophila* infection (Arasaki et al., 2012; Ingmundson et al., 2007; Machner and Isberg, 2006; Mukherjee et al., 2011; Müller et al., 2010; Murata et al., 2006; Neunuebel et al., 2011; Tan and Luo, 2011).

Ubiquitination regulates all aspects of eukaryotic cell physiology, and therefore is exploited by various bacterial pathogens encoding ubiquitin (Ub) ligases and deubiquitinases (DUBs) (Ashida and Sasakawa, 2017; Kitao et al., 2020; Kubori et al., 2019; Lin and Machner, 2017). Effector-mediated Ub modification of Rab1 was reported as an action of the *Legionella* E3 ligase SidC and its paralog SdcA (Horenkamp et al., 2014). Rab33b as well as Rab1, Rab6A, and Rab30 are conjugated with phosphoribosylated (PR)-Ub by the unique reaction mechanism of the SidE family of effector proteins (Qiu et al., 2016), and it was shown that recruitment of Rab33b and Rab6A to the *Legionella*-containing vacuole (LCV) relies on the PR-ubiquitination of Rab33b (Kawabata et al., 2021). A recent genome-wide screen identified host factors including Rab10 linked to intracellular replication of *L. pneumophila* (Jeng et al., 2019). It was demonstrated that Rab10 is recruited to the LCV and is ubiquitinated depending on the activity of SidC and SdcA (Jeng et al., 2019; Liu et al., 2020).

SidC and SdcA were originally identified as tethering factors that function in ER-to-LCV trafficking both having a unique phosphatidylinositol-4 phosphate (PI[4]P)-binding domain (Ragaz et al., 2008). The enzymatic activity of these proteins as Ub ligases was experimentally uncovered later (Hsu et al., 2014). The enzymatic activity was found to be encoded in the domain conserved between the two proteins, namely SidC N-terminal Ub ligase (SNL) domain (Hsu et al., 2014). SdcB (Lpg2452/LegA14) was identified as

another *L. pneumophila* Ub ligase having the SNL domain (Lin et al., 2018). However, the role of SdcB in *L. pneumophila* infection has not been examined yet.

Various *L. pneumophila* effector proteins exploit the host Ub signaling cascade (Kitao et al., 2020; Luo et al., 2021; Tomaskovic et al., 2022). They are exemplified by MavC which was shown to chemically modify the E2 enzyme UBE2N. The transglutaminase activity of MavC catalyzes a covalent linkage between Ub and UBE2N, thereby abolishing the activity of UBE2N to form polyUb chains, and mediate host NFκB signaling (Gan et al., 2019a). Encoded by the neighboring gene of *mavC*, MvcA is a paralog of MavC and exhibits similar activity to MavC as a Ub-specific deamidase (Valleau et al., 2018). However, MvcA was found to have an ability to reverse MavC-mediated Ub conjugation to UBE2N by its unique DUB activity (Gan et al., 2020). The enzymatic activities of MavC and MvcA are both inhibited by Lpg2149, an effector encoded downstream of *mvcA*, by blocking their catalytic residues (Valleau et al., 2018).

In this study, we investigated the role of *Legionella* Ub ligases in Rab10 dynamics during *L. pneumophila* infection. Including the unexpected finding that MavC is a negative regulator of SdcB, we demonstrated muti-tiered regulation by many effectors to finely modulate the localization of Rab10 to the LCV, revealing the intricate effector network that hijacks cellular processes.

Results

The SidE- and SidC-family proteins differentially contribute to ubiquitination of Rab10 in infected cells

Host Rab10 is required for optimal intracellular replication of *L. pneumophila* (Jeng et al., 2019) and therefore considered to play a significant role in LCV biogenesis or maintenance. Since *L. pneumophila* SidE family proteins, which catalyze PR-linked ubiquitination, have a wide range of substrates including Rab1 and Rab33b (Bhogaraju et al., 2016; Kalayil et al., 2018; Kotewicz et al., 2017; Qiu et al., 2016), we first examined whether the SidE family can affect Rab10 ubiquitination. Upon infection of HEK293T-FcγRII cells transiently expressing FLAG-Rab10 and HA-Ub with a wild-type *L. pneumophila* strain (Lp01), Rab10 was detected with a shifted band of higher molecular mass (Figure 1a upper panel). The band was shown to contain Ub by probing with an anti-HA antibody (Figure 1a lower panel), indicating that the band represents Rab10 conjugated with a single Ub molecule. The mass shift was not detected in cells infected

with the T4SS-deficient strain (Δ*dotA*), suggesting that Rab10 can be monoubiquitinated in a T4SS-dependent manner. Infection with a Δ*sidEs* strain lacking all four SidE-family proteins (SidE, SdeA, SdeB and SdeC) mostly eliminated the molecular mass shift of Rab10, while infection with a strain lacking the negative regulators of SidE family proteins (DupA, DupB, SidJ and SdjA (Black et al., 2019; Gan et al., 2019b; Qiu et al., 2017; Shin et al., 2020; Sulpizio et al., 2019)) enhanced the intensity of the band (Figure 1a). These results suggest that the SidE-family proteins can conjugate PR-Ub to Rab10. The high molecular weight smears detected with anti-HA antibody are thought to be polyUb chains (Figure 1a lower panel). Appearance of these smears is tightly associated with the PR-Ub bands, showing that polyubiquitination of Rab10 is linked with its PR-ubiquitination.

To examine if PR-Ub conjugation to Rab10 can enhance its modification with polyUb chains, we infected HEK293T-FcγRII cells expressing FLAG-Rab10 and HA-Ub with the Δ*sidEs* strain complemented with a plasmid expressing wild-type or a catalytic mutant of SdeA ($SdeA_{EE/AA}$), a representative SidE-family protein (Figure 1b). We detected a strongly enhanced polyUb smear whose appearance depends on the mono-ADP ribosyltransferase activity of SdeA. The intensity of the monoubiquitination band was correlated with that of the polyUb smears (Figure 1b middle panel). When the C-terminal GG motif of Ub was replaced with AA (Ub_{AA}), the polyUb smear drastically diminished, and accumulation of monoUb-conjugated Rab10 was observed instead. This indicates that the polyUb chains on Rab10 were formed via the Ub C-terminus by the canonical ubiquitination reaction. This also shows that the observed monoUb-conjugation to Rab10 does not require the Ub C-terminus, which is consistent with the formation of bridge between Arg42 of Ub and substrate catalyzed by the SidE effectors (Bhogaraju et al., 2016; Kotewicz et al., 2017; Qiu et al., 2016). These results strongly support that Rab10 is subjected to SdeA-mediated PR-ubiquitination and that this modification may provide a platform of conjugation of polyUb chains to Rab10, which is expected to be mediated by other Ub ligases.

Since it was reported that *L. pneumophila* effectors SidC and its paralog SdcA induce Rab10 ubiquitination (Jeng et al., 2019; Liu et al., 2020), we investigated how these E3 ligases contribute towards ubiquitination of Rab10 in our system (Figure 1c). Infection of cells with a Δ*sidC*Δ*sdcA* strain as well as with a strain lacking all the SidC family proteins (Δ*sidC*Δ*sdcA*Δ*sdcB*) still caused both mono- and polyubiquitination of Rab10 but with reduced levels. On the contrary, infection with the Δ*sidEs* strain eliminated both

139 modifications. These results support that SidE-family proteins primarily contribute
140 towards ubiquitination of Rab10, and that SidC-family proteins partly contribute towards
141 polyubiquitination of Rab10 directly or indirectly in conditions where Rab10 is modified
142 with PR-Ub.
143

144 **Rab10 recruitment to the LCV is differentially regulated by SidE- and SidC-family**
145 **proteins**

146 Earlier studies demonstrated that Rab10 ubiquitination is highly correlated with its
147 localization to the LCV (Jeng et al., 2019; Liu et al., 2020). We therefore examined if the
148 SidE family regulates Rab10 recruitment to the LCV using HeLa-FcγRII cells transiently
149 expressing RFP-Rab10 (Figure 2a and b). Infection with the Δ*sidEs* strain drastically
150 reduced the level of Rab10-positive LCVs at all time points examined (Figure 2b). As
151 reported for Rab33b (Kawabata et al., 2021), PR-ubiquitination is thought to be required
152 for Rab10 to localize to the LCV. The Δ*sidC*Δ*sdcA* LCV also exhibited a reduced the
153 level of Rab10 localization at 1 h after infection (Figure 2b left panel). However, the level
154 of Rab10 recruitment to the Δ*sidC*Δ*sdcA* LCV recovered at 4 h after infection, while that
155 to the Δ*sidC*Δ*sdcA*Δ*sdcB* LCV did not recover even as late as 7 h (Figure 2b middle and
156 right panels). This result suggests that SdcB can contribute towards retention of Rab10
157 on the LCV at late stages of infection.
158

159 **SdcB associates with the LCV and plays a major role in Ub recruitment to the LCV**
160 **at late stages of infection**

161 The Ub accumulation on the LCV has been thought to be mediated largely by SidC and
162 SdcA (Horenkamp et al., 2014; Luo et al., 2015). We therefore examined the possible role
163 of SdcB in Ub recruitment to the LCV at distinct time points after infection (Figure 3).
164 To mask the effect of SidC and SdcA, we used a Δ*sidC*Δ*sdcA*Δ*sdcB* strain complemented
165 with wild-type or catalytic mutant (C57A) of SdcB expressed from a plasmid. When
166 HeLa-FcγRII cells were infected with these strains for 1 h, SdcB was detected around the
167 LCV (Figure 3a and b). The level of wild-type SdcB-positive LCVs was relatively lower
168 compared with that of the $SdcB_{C57A}$-positive LCVs, probably due to its catalytic cycling.
169 The expression of wild-type SdcB led to recruitment of Ub to the vacuole even without
170 SidC and SdcA, while expression of $SdcB_{C57A}$ did not (Figure 3b). This result indicates
171 that SdcB has a catalytic activity to conjugate Ub to substrates on the LCV. At 7 h after
172 infection, the level of the SdcB-positive LCVs was elevated to about 70 % regardless of
173 its catalytic activity (Figure 3c and d). At this time point, the level of the Ub-positive
174 LCVs was also raised to about 60 %, but only when SdcB was catalytically active. These

175 results demonstrate that SdcB can play a substantial role to conjugate Ub to substrates on
176 the LCV at late stages of infection.
177
178 **The catalytic activity of SdcB enhances retention of Rab10 on the LCV**
179 To examine the relationship between the catalytic activity of SdcB and the LCV
180 localization of Rab10, we assessed the level of Rab10-positive LCVs on which SdcB
181 localized. At 7 hs post infection, Rab10 localization was readily detected on
182 Δ*sidC*Δ*sdcA*Δ*sdcB* LCVs containing wild-type SdcB, but not the inactive $SdcB_{C57A}$
183 mutant (Figure 4a). The level of Rab10-positive LCVs was significantly higher with
184 expression of wild-type SdcB than that of the catalytic mutant (Figure 4b), suggesting
185 that the Ub ligation activity of SdcB supports retention of Rab10 on the LCV until late
186 stages of infection.
187
188 **MavC modifies SdcB when ectopically expressed in cells**
189 A potential relationship between SdcB and MavC as an effector/metaeffector pair was
190 suggested by a recent systematic analysis utilizing yeast genetics (Urbanus et al., 2016).
191 We therefore examined whether expression of MavC can affect the activity profile of
192 SdcB in cells. When ectopically expressed in HEK293T-FcγRII cells, 3xFLAG-tagged
193 SdcB could not be detected (Figure 5a top panel, most left lane). However, we found that
194 coexpression of GFP-tagged MavC, but not of its catalytic mutant ($MavC_{C74A}$), recovered
195 the detection of SdcB (Figure 5a top panel). As SdcB was resolved as a doublet in the
196 immunoblot, we suspected that SdcB may be chemically modified by MavC and that the
197 modification may result in enhanced detection of this protein. We therefore probed with
198 an anti-HA antibody to detect possible Ub conjugation. The upper band was stained with
199 anti-HA antibody, showing that Ub was conjugated to SdcB presumably by the known
200 Ub conjugation ability of MavC (Gan et al., 2019a) (Figure 5a middle panel). We also
201 found that the disappearance of the SdcB bands correlated with the appearance of the high
202 molecular weight smears when probed with anti-HA antibody (Figure 5a middle panel).
203 This suggests that the disappearance of the SdcB band can be caused by auto-
204 ubiquitination, as SdcB has an ability to catalyze auto-ubiquitination with a diverse
205 repertoire of E2 enzymes (Figure 5-figure supplement 1) consistently with a previous
206 report (Lin et al., 2018). The transglutaminase activity of MavC is likely required for
207 conjugation of Ub to SdcB, as the catalytic mutant of MavC ($MavC_{C74A}$) failed to modify
208 SdcB (Figure 5a). We also found that unmodified SdcB was readily detected when the
209 SdcB C57 active site was mutated regardless of the presence of MavC (Figure 5b top
210 panel), consistent with the disappearance of the band was caused by the auto-

211 ubiquitination. Interestingly, the MavC-mediated Ub conjugation to $SdcB_{C57A}$ was not
212 readily detected (Figure 5b). This indicates that the catalytic residue C57 of SdcB is
213 crucial in being modified by MavC. As suggested by the reduction of the high molecular
214 weight smears (Figure 5a), it is plausible that MavC suppresses the E3 ligase activity of
215 SdcB by the unique chemical modification.
216
217 **The transglutaminase activity of MavC mediates Ub conjugation to SdcB and to**
218 **SdcA**
219 To confirm the direct involvement of MavC in the unique Ub modification of SdcB, we
220 reconstructed an *in vitro* reaction using purified proteins. In the presence of MavC, but
221 not of its paralog MvcA, the mass shift of SdcB was readily detected (Figure 5c top panel).
222 The immunoblotting showed that the band contains Ub (Fig. 5C middle panel). The
223 presence of wild-type MavC, but not its catalytic mutant, also reduced SdcB auto-
224 ubiquitination *in vitro* (Figure 5-figure supplement 2). Since SidC, SdcA and SdcB are
225 paralogs to each other, we examined if SidC and/or SdcA are also subject to MavC-
226 mediated Ub conjugation. Triple-FLAG-tagged SidC or SdcA were transiently expressed
227 together with GFP-MavC and HA-Ub in HEK293T-FcγRII cells, and the 3xFLAG-tagged
228 proteins were immunoprecipitated (Figure 5d). These results clearly demonstrated that
229 Ub was conjugated to SdcA but not to SidC by the catalytic activity of MavC, and that
230 this modification occurred only to SdcA in the catalytically active form.
231
232 We then analyzed the MavC-mediated Ub-conjugation to SdcB using derivatives of Ub
233 (Figure 5e and f). The use of Ub having no Lys residues (HA-$Ub_{No\ K}$) resulted in an
234 enhanced level of Ub-conjugation to SdcB mediated by functional MavC (Figure 5e
235 middle panel). Surprisingly, HA-Ub_{AA} did not conjugate to SdcB, indicating that the C-
236 terminal Gly-Gly residues are essential for MavC-mediated Ub conjugation to SdcB
237 (Figure 5f middle panel). The shifted band detected by FLAG probing plausibly
238 represents conjugation of cellular intrinsic Ub (Figure 5f top panel).
239
240 Transglutaminase activity of MavC is known to target Gln40 of Ub to catalyze the
241 intramolecular crosslinking (Gan et al., 2019a; Guan et al., 2020; Puvar et al., 2020). We
242 investigated whether the same residue of Ub is crosslinked to SdcB by the activity of
243 MavC using mass spectrometric (MS) analysis. We found that a covalent bond was
244 formed between Gln41 of Ub and Lys518 of SdcB (Figure 6a). Crosslinking between
245 Gln31 of Ub and Lys891 of SdcB was also detected (Figure 6-figure supplement 1). To
246 confirm the results, we replaced Ub residues Gln41 and Gln31 with Glu (Ub_{Q41E}, Ub_{Q31E},

247 and Ub $_{Q31E\ Q41E}$) and conducted the Ub-conjugation assay by transient expression in
248 HEK293T-FcγRII cells. Consistent with the result from the MS analysis, Ub $_{Q41E}$, but not
249 Ub $_{Q40E}$, failed to be conjugated to SdcB, showing that Gln41 is crucial for MavC-
250 mediated crosslinking with SdcB (Figure 6b middle panel). Ub $_{Q31E}$ also reduced the level
251 of modified SdcB, and Ub $_{Q31E\ Q41E}$ completely abolished the crosslinking to SdcB. The
252 presence of modified SdcB bands when probed with anti-FLAG antibody is thought to be
253 caused by conjugation with intrinsic Ub in cells (Figure 6b top panel). Contrarily,
254 replacement of Lys518 and Lys891 of SdcB to Arg (SdcB $_{K518R}$, SdcB $_{K891R}$, and SdcB
255 $_{K518R\ K891R}$) showed lesser impact on abolishing the reactivity (Figure 6c), suggesting that
256 additional residues of SdcB can be subjected to MavC-dependent Ub conjugation. Taken
257 together, we currently hypothesize that association of the C-terminal Gly of Ub to the
258 catalytic pocket of SdcA or SdcB (C44 or C57, respectively) positions these molecules in
259 proper orientation for intramolecular crosslinking mediated by the transglutaminase
260 activity of MavC.
261
262 **Catalytic activity of MavC can impact Rab10 localization to the LCV**
263 We then examined the role of MavC in the LCV localization of Rab10. By
264 immunofluorescent microscopy, we monitored the level of RFP-tagged Rab10 on SdcB-
265 positive LCVs when MavC or its catalytic mutant were expressed in HeLa-FcγRII cells
266 (Figure 7a). At 4 h after infection with *L. pneumophila* strains expressing 3xFLAG-SdcB,
267 the level of Rab10-positive LCVs was significantly higher in the cells expressing the
268 catalytic mutant of MavC compared with those expressing wild-type MavC (Figure 7a
269 and b). That Rab10 localization was reduced coincident with MavC-dependent inhibition
270 of SdcB further supports the contribution of SdcB activity towards retention of Rab10 on
271 the LCV. We then wondered whether bacterially delivered MavC can contribute to the
272 elimination of Rab10 from the vacuole. As the levels of the Rab10-positive LCVs were
273 not significantly altered up to 7 h after infection with the wild-type *L. pneumophila* strain
274 (Figure 2b), we examined Rab10 localization at a later time point after infection (Figure
275 7c, Figure 7-figure supplement 1). At 9 h after infection, the level of Rab10-positive
276 LCVs was significantly higher in the cells infected with a Δ*mavC*Δ*mvcA* strain than with
277 the wild-type strain. Contrary, when the cells were infected with a strain lacking Lpg2149
278 which inhibits the activity of MavC and MvcA [31], the level declined. These results
279 supports that MavC suppresses the activity of SdcB in infection conditions and thereby
280 downregulates Rab10 localization to the LCV at late stages of infection (Figure 7d).
281
282 **Discussion**

283 Following the finding that subversion of Rab1 function is critical for *L. pneumophila* to
284 create the replicative vacuole (Kagan et al., 2004), remarkable numbers of studies have
285 revealed the molecular mechanisms of how *L. pneumophila* T4SS effectors modulate the
286 localization and enzymatic activity of Rab1 (Qiu and Luo, 2017). The importance of
287 Rab10 and its chaperone *RABIF* for intracellular replication of *L. pneumophila* has
288 recently emerged (Jeng et al., 2019). However, little is known about how *L. pnuemophila*
289 manipulates the activity of Rab10.
290
291 We found that the SidE-family effectors mediate noncanonical ubiquitination of Rab10.
292 Apparently, this modification is the primary requirement for subsequent
293 polyubiquitination of Rab10 (Figure 1), which is linked to its localization to the LCV
294 (Figure 2). Polyubiquitination of Rab10 was enhanced in a manner depending on the
295 catalytic activities of the SidC-family proteins (Figure 1) consistent with previous reports
296 (Jeng et al., 2019; Liu et al., 2020). As ectopic expression of SdeA in HEK293T-FcγRII
297 cells led to monoubiquitination of Rab10 (Figure 7-figure supplement 2), it is plausible
298 that PR-Ub conjugation to Rab10 is directly catalyzed by the SidE-family ligases.
299 However, the SdcB-mediated polyubiquitination of Rab10 was not readily detected even
300 in the presence of SdeA lacking its DUB domain (Figure 7-figure supplement 2). This
301 result prompted us to consider that polyubiquitination of Rab10 can be partly catalyzed
302 by canonical E3 ligases in host cells and/or other *L. pneumophila* effector proteins. The
303 Ub ligase activity of SdcB strongly induced accumulation of Ub on the LCV (Figure 3).
304 The PR-Ub modification of Rab10 and ubiquitination of unknown LCV-associated
305 substrates of the SidC family may provide the platform for the further modification of
306 Rab10.
307
308 Involvement of MavC for regulation of the SidC-family ligases was unexpectedly
309 identified in our analyses. This finding has added another layer of complexity to effector-
310 mediated regulation of Rab10. It was previously demonstrated that MavC can catalyze
311 covalent linkage between Q40 of Ub with a Lys residue of UBE2N (Gan et al., 2019a).
312 Our result showing that Q41 of Ub is crosslinked with SdcB gives a new insight into the
313 molecular mechanism of how MavC catalyzes Ub conjugation to specific substrates. In
314 addition, both the C-terminal Gly of Ub (Figure 5f) and the catalytic Cys of SdcB (C57A)
315 (Figure 5b) were essential for crosslinking. This strongly suggests that the ability of SdcB
316 as a Ub ligase to position a Ub molecule into its active site is a requirement for MavC to
317 form the covalent bond between Ub and SdcB. This model is reminiscent of the reaction
318 scheme described for how MavC mediates Ub conjugation to UBE2N, in which the initial

319 capturing of Ub by the E2 activity of UBE2N allows enhanced activity by MavC (Puvar
320 et al., 2020).
321
322 In contrast to the PI[4]P-binding domain present in SidC and SdcA, SdcB has an ankyrin
323 repeat (ANK) domain at its C-terminus. As ANK domains are generally known to mediate
324 protein-protein interactions, we speculate that SdcB targets substrates distinct from those
325 of SidC and SdcA. The lipid-binding ability of SidC and SdcA implicates their substrate
326 specificity; their substrates are on or associated with the LCV in the specific stages of
327 vacuole remodeling (Vormittag et al., 2023). We, therefore, speculate that SdcB can target
328 substrate(s) present on the LCV in maturation stages different from ones when SidC and
329 SdcA can work in. In spite of our extensive efforts, we have not succeeded to identify
330 cellular targets with which the ANK domain of SdcB interacts. It would be a future
331 perspective to understand the exact biological role of SdcB as a Ub ligase in *L.*
332 *pneumophila* infection by identifying its enzymatic substrates.
333
334 We found that *L. pneumophila* has a multi-tiered regulatory mechanism to manipulate Ub
335 signaling cascades in which SidC- and SidE-family Ub ligases are involved. MavC was
336 found to contribute to fine-tuning the regulation via its unique Ub-conjugation activity
337 toward SdcB. These regulations are reflected in many aspects of the LCV biogenesis and
338 maturation which are thought to be largely controlled by Ub signaling. The regulatory
339 cascade of Rab10 GTPase, whose function is crucial for ER recruitment to the LCV,
340 became apparent in this study. Most likely, similar regulatory cascades exist for many
341 LCV-associated proteins.
342
343 **Materials and methods**
344
345 **Bacterial strains and growth conditions**
346 The *L. pneumophila* and *Escherichia coli* strains used in this study are listed in Key
347 resource table. Deletion strains were constructed by allelic exchange, as described
348 previously (Zuckman et al., 1999). The *L. pneumophila* strains were grown at 37°C in
349 liquid N-(2-acetamido)-2-aminoethanesulfonic acid (ACES; Sigma)-buffered yeast
350 extract (AYE) media or on charcoal-yeast extract (CYE) plates (Feeley et al., 1979) with
351 or without appropriate antibiotics (100 µg /mL streptomycin, 10 µg/mL chloramphenicol,
352 and 10 µg/mL kanamycin), as described previously (Berger et al., 1994). The *Eschericia*
353 *coli* strains (DH5α, DH5αλpir, and BL21[DE3]) were grown at 37°C in standard media.
354

355 **Cell culture**
356 HeLa-FcγRII cells (Arasaki et al., 2017) were grown in Minimum Essential Medium α
357 (MEMα; Gibco) supplemented with 10% fetal bovine serum (FBS; Sigma). HEK293T-
358 FcγRII cells (Arasaki and Roy, 2010) were grown in Dulbecco's Modified Eagle
359 Medium (DMEM; Gibco) supplemented with 10% FBS. All cells were incubated at
360 37ºC under 5% CO_2 condition.
361
362 **Plasmid construction**
363 Plasmids used in this study are listed in Appendix 1-table 1. All cloning was conducted
364 by PCR-amplification of the desired genes using primers listed in Appendix 2-table 2
365 from genomic DNA of *L. pneumophila* or from plasmids listed in Appendix 2-table 2
366 followed by ligation with the vectors unless otherwise noted below. Site-directed
367 mutagenesis was carried out using a QuickChange II site-directed mutagenesis Kit
368 (Agilent) according to the manufacture's recommendation. For construction of pET15b-
369 His-*sdeA*$_{\Delta DUB}$, the entire region of pET15b-His-*sdeA* except for the region encoding 1-
370 199 aa of SdeA was amplified with primers 2649/2712 and then the fragment was self-
371 ligated with a Gibson assembly kit (New England Biolabs). For construction of pmGFP-
372 *sdeA*$_{\Delta DUB}$, the entire region of pmGFP-*sdeA* except for the region encoding 1-199 aa of
373 SdeA was amplified with primers 2714/2715 and then the fragment was self-ligated with
374 a Gibson assembly kit. For construction of pMMB-3xMyc-*sdeA*, the coding region of
375 *sdeA* was amplified using primers 2658/2659 from genomic DNA of Lp01, then the
376 fragment was ligated with a linearized vector generated by PCR using 2341/2681 based
377 on pMMB-PicmR-3xFLAG.
378
379 **Protein purification**
380 *E. coli* cells overproducing MavC, MvcA or SdcB with a hexa-histidine tag were collected
381 by centrifugation and resuspended with 50 mM Tris-HCl pH 7.5, 5 mM EDTA containing
382 SigmaFast Protease Inhibitor Cocktail (Sigma). Cells were disrupted, centrifuged (30,000
383 × *g*, 20 min), and the soluble fraction was loaded on a HiPrep Q FF column (Cytiva). His-
384 tagged MacV or MvcA was eluted by a 0-500 mM gradient of NaCl in 20 mM Tris-HCl
385 pH7.5, 10 mM 2-mercaptoethanol and was loaded on a HisTrap HP column (Cytiva). His-
386 tagged protein was eluted by a 40-500 mM gradient of imidazole in 20 mM Tris-HCl pH
387 7.5, 200 mM NaCl, 10 mM 2-mercaptoethanol. Peak fractions were pooled and loaded
388 onto a HiLoad Superdex 200 gel filtration column (Cytiva). Purified protein was eluted
389 in 20 mM Tris-HCl pH 7.5, 200 mM NaCl, 1mM dithiothreitol and concentrated using a
390 Vivaspin 20 concentrator (Sartorius).

391

392 **Ub ligation assay**

393 The *in vitro* ubiquitination assay in the substrate-free system was conducted as described
394 before (Kubori et al., 2018) with minor modifications. Briefly, reaction mixtures (12.5 μl)
395 containing 5 μg of recombinant human Ub (Boston Biochem), 80 nM recombinant human
396 E1 (Boston Biochem), 400 nM recombinant human E2 enzymes (Boston Biochem) and
397 400 nM purified E3 ligases in 50 mM Tris-Cl (pH 7.5), 2 mM $MgCl_2$, 120 mM NaCl, 2
398 mM ATP and 1 mM DTT were incubated for 2 h at 30°C. The reaction was stopped by
399 adding 12.5 μl of 2xSDS sample buffer and boiling.

400

401 **Transglutaminase assay**

402 The *in vitro* transglutaminase assay was conducted using the same buffer for the Ub
403 ligation assay (omitting ATP). Reaction mixtures (12.5 μl) containing 5 μg of Ub, 400 nM
404 purified His-SdcB and 800 nM purified MavC were incubated for 1 h at 37°C. The
405 reaction was stopped by adding 12.5 μl of 2xSDS sample buffer and boiling.

406

407 **Transfection and infection**

408 HEK293T-FcγRII cells were seeded in poly-L-lysine (Sigma)-coated 6-well tissue culture
409 plates at 6×10^5 cells/well 24 h before transfection or infection. Transfection was
410 performed using Lipofectamine2000 (Invitrogen) for 24 h according to the
411 manufacturer's recommendation. HeLa-FcγRII cells were seeded on coverslips in 24-well
412 tissue culture plates at 4×10^4 cells/well 24 h before transfection or infection. Transfection
413 was performed using Polyethylenimine (PEI) for 24 hr. For infection, *L. pneumophila*
414 was harvested from a 2-days heavy patch grown on CYE plates with or without
415 appropriate antibiotics and 1 mM IPTG, and then it was resuspended in sterilized distilled
416 water. The bacteria were opsonized with anti-*Legionella* antibody (1:3,000 dilution)
417 before infection. After adding the bacteria to the cells, the plates were centrifuged at 200
418 × g to precipitate bacteria onto the layer of cells and were immediately warmed in a 37°C
419 water-bath by floating for 5 min and then placed in a CO_2 incubator at 37°C. At 1 h after
420 infection, the infected cells were washed three times with prewarmed Dulbecco's
421 Phosphate Buffered Saline (DPBS; Sigma) and refreshed with prewarmed media to
422 remove the extracellular bacteria, and incubation was resumed at 37°C in a CO_2 incubator.

423

424 **Immunoprecipitation**

425 The transfected or infected cells were washed with DPBS three times and lysed with Lysis
426 buffer (20 mM Tris-HCl, pH 7.5, 150 mM NaCl, 1 mM EDTA, 1% NonidentP40)

427 containing protease inhibitors (cOmplete; Roche), 1 mM phenylmethylsulfonyl
428 fluoride (PMSF; Nacarai), 10 mM N-Ethylmaleimide (NEM, Sigma) as a DUB inhibitor
429 and 10 μM MG132 (Calbiochem) as a proteasome inhibitor. After removal of cell debris
430 with centrifugation, cell lysates were incubated with FLAG M2 magnetic beads (Sigma)
431 or RFP-Trap magnetic beads (chromotek) for 2 h to overnight at 4°C. The beads were
432 washed five times with wash buffer (20 mM Tris-HCl, pH 7.5, 150 mM NaCl, 1mM
433 EDTA, 0.1% TritonX-100), and the bead-bound proteins were eluted by boiling in SDS
434 sample buffer.
435
436 **Immunofluorescent microscopy**
437 HeLa-FcγRII cells on coverslips were fixed with 4% paraformaldehyde /DPBS for 20
438 min at room temperature and washed with DPBS three times. After permeabilization and
439 blocking with 0.2 % Triton X-100 and 2 % goat serum in DPBS for 20 min, the coverslips
440 were incubated with the primary antibodies indicated in the figure legends for 90 min.
441 After washing with DPBS three times, the coverslips were incubated with the fluorescent
442 secondary antibodies with DAPI for 40 min. After washing with DPBS three times, the
443 coverslips were mounted on glass slides using ProLong Diamond antifade mounting
444 medium (Thermo Fisher). Images were collected using an inverted microscope (TE2000-
445 U; Nikon) equipped with a digital ORCA-ERA camera (Hamamatsu).
446
447 **LC-MS/MS analysis**
448 Protein bands corresponding to MavC-mediated modification of 3xFLAG-SdcB were
449 excised from SDS-PAGE and digested with trypsin. Mass spectrometry experiments were
450 performed at the Research Institute for Microbial Diseases (RIMD). The proteins were
451 reduced with 10 mM DTT, followed by alkylation with 55 mM iodoacetamide, digested
452 by treatment with trypsin (Promega) and purified with a C18 tip (AMR, Tokyo, Japan).
453 The resultant peptides were subjected to nanocapillary reversed-phase LC-MS/MS
454 analysis using a C18 column (12 cm x 75 um, 1.9μm, Nikkyo technos, Tokyo, Japan) on
455 a nanoLC system (Bruker Daltoniks, Bremen, Germany) connected to a timsTOF Pro
456 mass spectrometer (Bruker Daltoniks) and a modified nano-electrospray ion source
457 (CaptiveSpray; Bruker Daltoniks). The mobile phase consisted of water containing 0.1%
458 formic acid (solvent A) and acetonitrile containing 0.1% formic acid (solvent B). Linear
459 gradient elution was carried out from 2% to 35% solvent B for 20 min at a flow rate of
460 250 nL/min. The ion spray voltage was set at 1.6 kV in the positive ion mode. Ions were
461 collected in the trapped ion mobility spectrometry (TIMS) device over 100 ms and MS
462 and MS/MS data were acquired over an m/z range of 100–2,000. During the collection of

MS/MS data, the TIMS cycle was adjusted to 0.53 s and included 1 MS plus 4 parallel accumulation serial fragmentation (PASEF)-MS/MS scans, each containing on average 12 MS/MS spectra (>100 Hz) (Meier et al., 2018, 2015) and nitrogen gas was used as collision gas.

The resulting data was processed using DataAnalysis version 5.2 (Bruker Daltoniks), resulting peak files (mgf format) were subjected to MASCOT version 2.7.0 (Matrix Science, London, UK) against the Swissprot_database(568,744 sequences; 205,548,017 residues) taxonomy limited homo sapiens (20,305 sequences), HA-Ub (1 sequences; 92 residues) and 3xFLAG-lpg2452 database (1 sequences; 950 residues), and searched with the following settings: The mass tolerance for precursor ions was ±15 ppm; The mass tolerance for fragment ions was ±0.05 Da; enzyme, Trypsin; max. missed cleavages, 4; fixed modification: carbamidomethylation on cysteine; variable modifications: oxidation of methionine, N-terminal Gln to pyro-Glu. The threshold score/expectation value for accepting individual spectra was $p < 0.05$. User defined Crosslinker setting is cross-linker: Ubiq01 (mass modification: -17.026549 Da, deamination). The cross-link reactions were assumed to connect Lysine or Glutamine. It does not pair with K and K, or Q and Q. It links only 3xFLAG-lpg2452 between HA-Ub.

Acknowledgements

We thank Tetsuya Honda, Masanari Nishikawa, Tenne Ichikawa, and Seryeong Du for their technical assistance. LC/MS-MS analysis was conducted by Akinori Ninomiya (Core Instrumentation Facility, Research Institute for Microbial Diseases, Osaka University, Japan). The 3xHA-Ub and 3xHA-Ub-AA expressing plasmids were kind gifts from Jiazhang Qiu (College of Veterinary Medicine, Jilin University, China). The HA-Ub expressing plasmid is a kind gift from Michinaga Ogawa (National Institute of Infectious Diseases, Japan). We thank Jonathan N. Pruneda (Department of Molecular Microbiology & Immunology, Oregon Health & Science University, USA) for providing a critical review of the manuscript. This study was supported by Takeda Science Foundation (to T. Ku.), MEXT/JSPS KAKENHI grants 22H02867 and 19H03469 (to T. Ku.), 20H05772 (to K. A.), 20K07477 (to T. Ki.), and 19H03470 (to H. N.).

Author contributions

Conceptualization, T. Ku.; Methodology, T. Ku., T. Ki., and K. A.; Investigation, T. Ku. and H. N.; Writing- Original Draft, T. Ku.; Writing-Review & Editing, T. Ku, H. N., and K. A.; Funding Acquisition, T. Ku., K. A., T. Ki, and H. N. Supervision, T. Ku. and H. N.

Declaration of interests

The authors declare no competing interests.

Figure legends

Figure 1. The SidE- and SidC-family proteins differentially contribute towards ubiquitination of Rab10.

HEK293T-FcγRII cells transiently expressing 3xFLAG-Rab10 and HA-Ub were infected with the indicated *L. pneumophila* strains for 1 h at an MOI of 20. Rab10 was isolated from cell lysate by immunoprecipitation using anti-FLAG magnetic beads and was probed with anti-FLAG and with anti-HA antibodies. Triple-HA-Ub (3xHA-Ub) or Ub in which the C-terminal GG were replaced with AA (3xHA-Ub_{AA}) was expressed instead of HA-Ub in (b). Bacterial lysates were probed with anti-Myc antibody in (b).

Figure 2. The SidE- and SidC-family proteins differentially contribute towards recruitment of Rab10 to the LCV.

HeLa-FcγRII cells transiently expressing RFP-Rab10 were infected with the indicated *L. pneumophila* strains at an MOI of 5 for 4 h (a) and for the indicated time (b). (a) Representative images of infected cells. Fixed cells were stained for *L. pneumophila* (green) and DNA (blue) and visualized with RFP-Rab10 (red). Magnified images in the white squares are shown in merged and in each channel. Arrows indicate the Rab10-positive LCVs. Scale bars, 10 μm. (b) Quantitation of Rab10-positive LCVs (%). Infections were performed in triplicate and each value represents scoring from 200 LCVs. Significance was determined using Student's t-test.

Figure 3. SdcB associates with the LCV and plays a major role in Ub recruitment to the LCV at late stages of infection.

HeLa-FcγRII cells were infected with the indicated *L. pneumophila* strains at an MOI of 2 for 1 h (a, b) and for 7 h (c, d). (a, c) Representative images of infected cells. Fixed cells were stained for FLAG-SdcB or Ub (green), *L. pneumophila* (red) and DNA (blue). Magnified images in the white squares are shown in the lower panels. Scale bars, 10 μm. (b, d) Quantitation of SdcB-positive (left) and of Ub-positive (right) LCVs (%). Infections

533 were performed in triplicate and each value represents scoring from 200 LCVs.
534 Significance was determined using Student's t-test.
535
536 **Figure 4. The catalytic activity of SdcB enhances retention of Rab10 on the LCV.**
537 HeLa-FcγRII cells transiently expressing RFP-Rab10 were infected with the indicated *L.*
538 *pneumophila* strains at an MOI of 2 for 7h. (a) Representative images of infected cells.
539 Fixed cells were stained for FLAG-SdcB (green) and DNA (*L. pneumophila*) (blue) and
540 visualized with RFP-Rab10 (red). Magnified images in the white squares are shown in
541 each channel. White arrows indicate the position of a bacterium. The red arrow indicates
542 a Rab10 signal surrounding an LCV. Scale bars, 10 μm. (b) Quantitation of Rab10-
543 positive LCVs (%) out of SdcB-positive ones. Infections were performed in triplicate and
544 each value represents scoring from 200 SdcB-positive LCVs. Significance was
545 determined using Student's t-test.
546
547 **Figure 5. The transglutaminase activity of MavC can mediate a unique Ub**
548 **conjugation to SdcB.**
549 (a) 3xFLAG-SdcB, HA-Ub and GFP-MavC were coexpressed in HEK293T-FcγRII cells.
550 SdcB was isolated from cell lysates by immunoprecipitation using anti-FLAG magnetic
551 beads and was probed with the indicated antibodies. The asterisks indicate the Ub-
552 conjugated form of SdcB. (b) 3xFLAG-SdcB and GFP-MavC were coexpressed in
553 HEK293T-FcγRII cells. SdcB was isolated from cell lysates by immunoprecipitation
554 using anti-FLAG magnetic beads and was probed with the indicated antibodies. The
555 asterisks indicate the Ub-conjugated form of SdcB. (c) *In vitro* transglutaminase assay
556 was performed using purified proteins. The samples were analyzed by SDS-PAGE
557 followed by silver staining (top) or by immunoblotting using the indicated antibodies
558 (middle and bottom). The asterisks indicate the Ub-conjugated form of SdcB. (d)
559 3xFLAG-SdcA or SidC, GFP-MavC and HA-Ub were coexpressed in HEK293T-FcγRII
560 cells. SdcA or SidC was isolated from cell lysates by immunoprecipitation using anti-
561 FLAG magnetic beads and was probed with the indicated antibodies. The asterisks
562 indicate the Ub-conjugated form of SdcA. (e) 3xFLAG-SdcB, GFP-MavC and HA-Ub or
563 Ub without any Lys residues ($Ub_{No\ K}$) were coexpressed in HEK293T-FcγRII cells. SdcB
564 was isolated from cell lysates by immunoprecipitation using anti-FLAG magnetic beads
565 and was probed with the indicated antibodies. The asterisks indicate the Ub-conjugated
566 form of SdcB. (f) 3xFLAG-SdcB, GFP-MavC and HA-Ub or Ub in which the C-terminal
567 GG were replaced with AA (Ub_{AA}) were coexpressed in HEK293T-FcγRII cells. SdcB
568 was isolated from cell lysates by immunoprecipitation using anti-FLAG magnetic beads

569 and was probed with the indicated antibodies. The asterisks indicate the Ub-conjugated
570 form of SdcB.
571
572 **Figure 6. Identification of residues on Ub and SdcB between which MavC can**
573 **crosslink.**
574 (a) MavC catalyzes the formation of an isopeptide bond between the Gln41 of Ub and the
575 Lys518 of SdcB. The indicated proteins were expressed in HEK293T-FcγRII cells and
576 SdcB was isolated from cell lysates by immunoprecipitation using anti-FLAG magnetic
577 beads. The samples were resolved by SDS-PAGE. The Ub-conjugated SdcB was detected
578 by immunoblotting and by CBB staining. The gel slices of areas of the bands shown with
579 the red squares were subjected to mass spectrometric analysis. Product ion spectrum was
580 shown for Ub peptide –AKIQDKEGIPPDQQR- crosslinked with SdcB peptide –
581 VLLDKEVNDEGIAEAVASK-. (b, c) The indicated proteins were coexpressed in
582 HEK293T-FcγRII cells. SdcB was isolated from cell lysates by immunoprecipitation
583 using anti-FLAG magnetic beads and was probed with the indicated antibodies. The
584 asterisks indicate the Ub-conjugated form of SdcB.
585
586 **Figure 7. Catalytic activity of MavC negatively regulates the Rab10 localization to**
587 **the LCV.**
588 (a, b) HeLa-FcγRII cells transiently expressing RFP-Rab10 and HA-MavC or its catalytic
589 mutant were infected with the Lp01 Δ*sidC* Δ*sdcA* Δ*sdcB* strain complemented with the
590 plasmid expressing 3xFLAG-SdcB or its catalytic mutant at an MOI of 2 for 4 h. (a)
591 Representative images of cells infected with the Lp01 Δ*sidC* Δ*sdcA* Δ*sdcB* strain
592 complemented with the plasmid expressing 3xFLAG-SdcB. Fixed cells were stained for
593 FLAG-SdcB (green) and DNA (blue), and visualized with RFP-Rab10 (red). Magnified
594 images in the white squares are shown in each channel. White arrows indicate the position
595 of a bacterium. The red arrow indicates a Rab10 signal surrounding an LCV. Scale bars,
596 10 μm. (b) Quantitation of Rab10-positive LCVs (%) out of SdcB-positive ones.
597 Infections were performed in triplicate and each value represents scoring from 200 SdcB-
598 positive LCVs. Significance was determined using Student's t-test. (c) HeLa-FcγRII cells
599 transiently expressing RFP-Rab10 were infected with the indicated Lp01 strains at an
600 MOI of 2 for 9 h, and Rab10-positive LCVs (%) were quantified. Infections were
601 performed in triplicate and each value represents scoring from 200 LCVs. Significance
602 was determined using Student's t-test. (d) The schematic of roles of SidE and SidC family
603 ligases in Rab10 localization to the LCV and of negative regulation of SdcB-dependent
604 Rab10 retention by the transglutaminase activity of MavC. Red arrows indicate canonical

605 Ub conjugation by SidC, SdcA and SdcB. Purple arrows indicate the noncanonical Ub
606 conjugation. In the early stage of infection, Rab10 is recruited to the LCV. This event is
607 linked to its PR-ubiquitination catalyzed by the SidE effectors. The PR-ubiquitination of
608 Rab10 provides a platform of its polyubiquitination in a manner depending on SidC and
609 SdcA. In later stages, SdcB contributes towards sustained Ub accumulation on the LCV,
610 retaining Rab10 on the vacuole (right). However, MavC-mediated crosslinking between
611 Ub and SdcB disrupts the catalytic activity of SdcB, resulting in releasing Rab10 from
612 the LCV (left).
613
614 **Figure 5-figure supplement 1. SdcB has a catalytic activity of self-ubiquitination**
615 **with preference of various E2 enzymes.**
616 Ub, E1 enzyme, indicated E2 enzymes and purified His-SdcB or His-SidC were mixed in
617 the reaction buffer in the presence of ATP and incubated at 30°C for 120 min. The samples
618 were analyzed by SDS-PAGE followed by silver staining (top) or by immunoblotting
619 using the anti-Ub antibody (bottom).
620
621 **Figure 5-figure supplement 2. The catalytic activity of MavC negatively impacts on**
622 **auto-ubiquitination of SdcB.**
623 Ub, E1 enzyme, His-UbcH6, purified His-SdcB and His-MavC were mixed in the
624 reaction buffer in the presence of ATP and incubated at 30°C for 120 min. The samples
625 were analyzed by SDS-PAGE followed by immunoblotting using the anti-Ub antibody.
626
627 **Figure 6-figure supplement 1. Mass spectrometry analysis identified additional**
628 **residues forming a covalent linkage between Ub and SdcB.**
629 Product ion spectrum was shown for Ub peptide –IQDKEGIPPDQQR- crosslinked with
630 SdcB peptide –GYVGVFFSGKENIK-.
631
632 **Figure 7-figure supplement 1. Bacterially delivered MavC mediates elimination of**
633 **Rab10 from the LCV.**
634 Representative images of cells infected with the indicated Lp01 strains at an MOI of 2 for
635 9 h (Rab10-positive LCVs (%) were quantified in Figure 7c). Fixed cells were stained for
636 *L. pneumophila* (green) and DNA (blue), and visualized with RFP-Rab10 (red).
637 Magnified images in the white squares are shown in each channel. Red arrows indicate
638 the Rab10 signal surrounding an LCV. Scale bars, 10 μm.
639
640 **Figure 7-figure supplement 2. Ectopic expression of SdcB does not proceed Rab10**

polyubiquitination even in the presence of SdeA.
Indicated proteins were coexpressed in HEK293T-FcγRII cells. Rab10 was isolated from cell lysates by immunoprecipitation using anti-RFP magnetic beads and was probed with the indicated antibodies. The asterisks indicate the Ub-conjugated form of Rab10.

Ethics statement

Not applicable.

QUANTIFICATION AND STATISTICAL ANALYSIS

In the immunofluorescence experiments, at least 200 bacterial vacuoles were counted per experiment. Student's t tests were carried out with data from three independent experiments.

References

Arasaki K, Mikami Y, Shames SR, Inoue H, Wakana Y, Tagaya M. 2017. Legionella effector Lpg1137 shuts down ER-mitochondria communication through cleavage of syntaxin 17. *Nat Commun* **8**. doi:10.1038/ncomms15406

Arasaki K, Roy CR. 2010. Legionella pneumophila promotes functional interactions between plasma membrane syntaxins and Sec22b. *Traffic* **11**:587–600. doi:10.1111/j.1600-0854.2010.01050.x

Arasaki K, Toomre DK, Roy CR. 2012. The legionella pneumophila effector DrrA is sufficient to stimulate SNARE-dependent membrane fusion. *Cell Host Microbe* **11**:46–57. doi:10.1016/j.chom.2011.11.009

Ashida H, Sasakawa C. 2017. Bacterial E3 ligase effectors exploit host ubiquitin systems. *Curr Opin Microbiol*. doi:10.1016/j.mib.2016.11.001

Berger KH, Merriam JJ, Isberg RR. 1994. Altered intracellular targeting properties associated with mutations in the Legionella pneumophila dotA gene. *Mol Microbiol* **14**:809–822. doi:10.1111/j.1365-2958.1994.tb01317.x

Bhogaraju S, Kalayil S, Liu Y, Bonn F, Colby T, Matic I, Dikic I. 2016. Phosphoribosylation of Ubiquitin Promotes Serine Ubiquitination and Impairs Conventional Ubiquitination. *Cell* **167**:1636-1649.e13. doi:10.1016/j.cell.2016.11.019

Black MH, Osinski A, Gradowski M, Servage KA, Pawłowski K, Tomchick DR, Tagliabracci VS. 2019. Bacterial pseudokinase catalyzes protein polyglutamylation to inhibit the SidE-family ubiquitin ligases. *Science (1979)* **364**:787–792. doi:10.1126/science.aaw7446

677 Feeley JC, Gibson RJ, Gorman GW, Langford NC, Rasheed JK, Mackel DC, Baine WB. 1979.
678 Charcoal-yeast extract agar: primary isolation medium for Legionella pneumophila. *J*
679 *Clin Microbiol* **10**:437–441. doi:10.1128/jcm.10.4.437-441.1979
680 Gan N, Guan H, Huang Y, Yu T, Fu J, Nakayasu ES, Puvar K, Das C, Wang D, Ouyang S,
681 Luo Z. 2020. Legionella pneumophila regulates the activity of UBE 2N by deamidase -
682 mediated deubiquitination . *EMBO J* **39**. doi:10.15252/embj.2019102806
683 Gan N, Nakayasu ES, Hollenbeck PJ, Luo ZQ. 2019a. Legionella pneumophila inhibits
684 immune signalling via MavC-mediated transglutaminase-induced ubiquitination of
685 UBE2N. *Nat Microbiol* **4**:134–143. doi:10.1038/s41564-018-0282-8
686 Gan N, Zhen X, Liu Yao, Xu X, He C, Qiu J, Liu Yancheng, Fujimoto GM, Nakayasu ES, Zhou
687 B, Zhao L, Puvar K, Das C, Ouyang S, Luo ZQ. 2019b. Regulation of phosphoribosyl
688 ubiquitination by a calmodulin-dependent glutamylase. *Nature* **572**:387–391.
689 doi:10.1038/s41586-019-1439-1
690 Guan H, Fu J, Yu T, Wang ZX, Gan N, Huang Y, Perčulija V, Li Y, Luo ZQ, Ouyang S. 2020.
691 Molecular Basis of Ubiquitination Catalyzed by the Bacterial Transglutaminase MavC.
692 *Advanced Science* **7**. doi:10.1002/advs.202000871
693 Horenkamp FA, Mukherjee S, Alix E, Schauder CM, Hubber AM, Roy CR, Reinisch KM. 2014.
694 Legionella pneumophila subversion of host vesicular transport by SidC effector proteins.
695 *Traffic* **15**:488–499. doi:10.1111/tra.12158
696 Hsu FS, Luo X, Qiu J, Teng Y Bin, Jin J, Smolka MB, Luo ZQ, Mao Y. 2014. The Legionella
697 effector SidC defines a unique family of ubiquitin ligases important for bacterial
698 phagosomal remodeling. *Proc Natl Acad Sci U S A* **111**:10538–10543.
699 doi:10.1073/pnas.1402605111
700 Hubber A, Roy CR. 2010. Modulation of host cell function by legionella pneumophila type IV
701 effectors. *Annu Rev Cell Dev Biol*. doi:10.1146/annurev-cellbio-100109-104034
702 Ingmundson A, Delprato A, Lambright DG, Roy CR. 2007. Legionella pneumophila proteins
703 that regulate Rab1 membrane cycling. *Nature* **450**:365–369. doi:10.1038/nature06336
704 Isberg RR, O'Connor TJ, Heidtman M. 2009. The Legionella pneumophila replication
705 vacuole: Making a cosy niche inside host cells. *Nat Rev Microbiol*.
706 doi:10.1038/nrmicro1967
707 Jeng EE, Bhadkamkar V, Ibe NU, Gause H, Jiang L, Chan J, Jian R, Jimenez-Morales D,
708 Stevenson E, Krogan NJ, Swaney DL, Snyder MP, Mukherjee S, Bassik MC. 2019.
709 Systematic Identification of Host Cell Regulators of Legionella pneumophila
710 Pathogenesis Using a Genome-wide CRISPR Screen. *Cell Host Microbe* **26**:551-563.e6.
711 doi:10.1016/j.chom.2019.08.017
712 Kagan JC, Stein MP, Pypaert M, Roy CR. 2004. Legionella Subvert the Functions of Rab1

713 and Sec22b to Create a Replicative Organelle. *Journal of Experimental Medicine*
714 **199**:1201–1211. doi:10.1084/jem.20031706
715 Kalayil S, Bhogaraju S, Bonn F, Shin D, Liu Y, Gan N, Basquin J, Grumati P, Luo ZQ, Dikic
716 I. 2018. Insights into catalysis and function of phosphoribosyl-linked serine
717 ubiquitination. *Nature* **557**:734–738. doi:10.1038/s41586-018-0145-8
718 Kawabata M, Matsuo H, Koito T, Murata M, Kubori T, Nagai H, Tagaya M, Arasaki K. 2021.
719 Legionella hijacks the host Golgi-to-ER retrograde pathway for the association of
720 Legionella-containing vacuole with the ER. *PLoS Pathog* **17**.
721 doi:10.1371/JOURNAL.PPAT.1009437
722 Kitao T, Nagai H, Kubori T. 2020. Divergence of Legionella Effectors Reversing Conventional
723 and Unconventional Ubiquitination. *Front Cell Infect Microbiol*.
724 doi:10.3389/fcimb.2020.00448
725 Kotewicz KM, Ramabhadran V, Sjoblom N, Vogel JP, Haenssler E, Zhang M, Behringer J,
726 Scheck RA, Isberg RR. 2017. A Single Legionella Effector Catalyzes a Multistep
727 Ubiquitination Pathway to Rearrange Tubular Endoplasmic Reticulum for Replication.
728 *Cell Host Microbe* **21**:169–181. doi:10.1016/j.chom.2016.12.007
729 Kubori T, Kitao T, Ando H, Nagai H. 2018. LotA, a Legionella deubiquitinase, has dual
730 catalytic activity and contributes to intracellular growth. *Cell Microbiol* **20**.
731 doi:10.1111/cmi.12840
732 Kubori T, Kitao T, Nagai H. 2019. Emerging insights into bacterial deubiquitinases. *Curr*
733 *Opin Microbiol*. doi:10.1016/j.mib.2018.10.001
734 Kubori T, Nagai H. 2016. The Type IVB secretion system: An enigmatic chimera. *Curr Opin*
735 *Microbiol*. doi:10.1016/j.mib.2015.10.001
736 Lin YH, Lucas M, Evans TR, Abascal-Palacios G, Doms AG, Beauchene NA, Rojas AL, Hierro
737 A, Machner MP. 2018. RavN is a member of a previously unrecognized group of
738 Legionella pneumophila E3 ubiquitin ligases. *PLoS Pathog* **14**.
739 doi:10.1371/journal.ppat.1006897
740 Lin YH, Machner MP. 2017. Exploitation of the host cell ubiquitin machinery by microbial
741 effector proteins. *J Cell Sci*. doi:10.1242/jcs.188482
742 Liu S, Luo J, Zhen X, Qiu J, Ouyang S, Luo ZQ. 2020. Interplay between bacterial
743 deubiquitinase and ubiquitin e3 ligase regulates ubiquitin dynamics on legionella
744 phagosomes. *Elife* **9**:1–23. doi:10.7554/eLife.58114
745 Luo J, Wang L, Song L, Luo ZQ. 2021. Exploitation of the Host Ubiquitin System: Means by
746 Legionella pneumophila. *Front Microbiol*. doi:10.3389/fmicb.2021.790442
747 Luo X, Wasilko DJ, Liu Y, Sun J, Wu X, Luo ZQ, Mao Y. 2015. Structure of the Legionella
748 Virulence Factor, SidC Reveals a Unique PI(4)P-Specific Binding Domain Essential for

749 Its Targeting to the Bacterial Phagosome. *PLoS Pathog* **11**.
750 doi:10.1371/journal.ppat.1004965
751 Machner MP, Isberg RR. 2006. Targeting of Host Rab GTPase Function by the Intravacuolar
752 Pathogen Legionella pneumophila. *Dev Cell* **11**:47–56.
753 doi:10.1016/j.devcel.2006.05.013
754 Meier F, Beck S, Grassl N, Lubeck M, Park MA, Raether O, Mann M. 2015. Parallel
755 accumulation-serial fragmentation (PASEF): Multiplying sequencing speed and
756 sensitivity by synchronized scans in a trapped ion mobility device. *J Proteome Res*
757 **14**:5378–5387. doi:10.1021/acs.jproteome.5b00932
758 Meier F, Brunner AD, Koch S, Koch H, Lubeck M, Krause M, Goedecke N, Decker J, Kosinski
759 T, Park MA, Bache N, Hoerning O, Cox J, Räther O, Mann M. 2018. Online parallel
760 accumulation–serial fragmentation (PASEF) with a novel trapped ion mobility mass
761 spectrometer. *Molecular and Cellular Proteomics* **17**:2534–2545.
762 doi:10.1074/mcp.TIR118.000900
763 Mukherjee S, Liu X, Arasaki K, McDonough J, Galán JE, Roy CR. 2011. Modulation of Rab
764 GTPase function by a protein phosphocholine transferase. *Nature* **477**:103–108.
765 doi:10.1038/nature10335
766 Müller MP, Peters H, Blümer J, Blankenfeldt W, Goody RS, Itzen A. 2010. The Legionella
767 Effector Protein DrrA AMPylates the Membrane Traffic Regulator Rab1b. *Science*
768 *(1979)* **329**:946–949. doi:10.1126/science.1192276
769 Murata T, Delprato A, Ingmundson A, Toomre DK, Lambright DG, Roy CR. 2006. The
770 Legionella pneumophila effector protein DrrA is a Rab1 guanine nucleotide-exchange
771 factor. *Nat Cell Biol* **8**:971–977. doi:10.1038/ncb1463
772 Neunuebel MR, Chen Y, Gaspar AH, Backlund PS, Yergey A, Machner MP. 2011. De-
773 AMPylation of the Small GTPase Rab1 by the Pathogen Legionella pneumophila.
774 *Science (1979)* **333**:453–456. doi:10.1126/science.1207193
775 Neunuebel MR, Machner MP. 2012. The taming of a Rab GTPase by Legionella
776 pneumophila . *Small GTPases* **3**:28–33. doi:10.4161/sgtp.18704
777 Puvar K, Iyer S, Fu J, Kenny S, Negrón Terón KI, Luo ZQ, Brzovic PS, Klevit RE, Das C.
778 2020. Legionella effector MavC targets the Ube2N~Ub conjugate for noncanonical
779 ubiquitination. *Nat Commun* **11**. doi:10.1038/s41467-020-16211-x
780 Qiu J, Luo ZQ. 2017. Legionella and Coxiella effectors: Strength in diversity and activity. *Nat*
781 *Rev Microbiol*. doi:10.1038/nrmicro.2017.67
782 Qiu J, Sheedlo MJ, Yu K, Tan Y, Nakayasu ES, Das C, Liu X, Luo ZQ. 2016. Ubiquitination
783 independent of E1 and E2 enzymes by bacterial effectors. *Nature* **533**:120–124.
784 doi:10.1038/nature17657

785 Qiu J, Yu K, Fei X, Liu Y, Nakayasu ES, Piehowski PD, Shaw JB, Puvar K, Das C, Liu X, Luo
786 ZQ. 2017. A unique deubiquitinase that deconjugates phosphoribosyl-linked protein
787 ubiquitination. *Cell Res* **27**:865–881. doi:10.1038/cr.2017.66
788 Ragaz C, Pietsch H, Urwyler S, Tiaden A, Weber SS, Hilbi H. 2008. The Legionella
789 pneumophila phosphatidylinositol-4 phosphate-binding type IV substrate SidC recruits
790 endoplasmic reticulum vesicles to a replication-permissive vacuole. *Cell Microbiol*
791 **10**:2416–2433. doi:10.1111/j.1462-5822.2008.01219.x
792 Sherwood RK, Roy CR. 2013. A rab-centric perspective of bacterial pathogen-occupied
793 vacuoles. *Cell Host Microbe*. doi:10.1016/j.chom.2013.08.010
794 Shin D, Mukherjee R, Liu Yaobin, Gonzalez A, Bonn F, Liu Yan, Rogov V V., Heinz M, Stolz
795 A, Hummer G, Dötsch V, Luo ZQ, Bhogaraju S, Dikic I. 2020. Regulation of
796 Phosphoribosyl-Linked Serine Ubiquitination by Deubiquitinases DupA and DupB.
797 *Mol Cell* **77**:164-179.e6. doi:10.1016/j.molcel.2019.10.019
798 Spanò S, Galán JE. 2018. Taking control: Hijacking of Rab GTPases by intracellular bacterial
799 pathogens. *Small GTPases*. doi:10.1080/21541248.2017.1336192
800 Sulpizio A, Minelli ME, Wan M, Burrowes PD, Wu X, Sanford EJ, Shin J-H, Williams BC,
801 Goldberg ML, Smolka MB, Mao Y. 2019. Protein polyglutamylation catalyzed by the
802 bacterial calmodulin-dependent pseudokinase SidJ. *Elife* **8**:e51162.
803 doi:10.7554/eLife.51162.001
804 Tan Y, Luo ZQ. 2011. Legionella pneumophila SidD is a deAMPylase that modifies Rab1.
805 *Nature* **475**:506–509. doi:10.1038/nature10307
806 Tomaskovic I, Gonzalez A, Dikic I. 2022. Ubiquitin and Legionella: From bench to bedside.
807 *Semin Cell Dev Biol*. doi:10.1016/j.semcdb.2022.02.008
808 Urbanus ML, Quaile AT, Stogios PJ, Morar M, Rao C, Di Leo R, Evdokimova E, Lam M,
809 Oatway C, Cuff ME, Osipiuk J, Michalska K, Nocek BP, Taipale M, Savchenko A,
810 Ensminger AW. 2016. Diverse mechanisms of metaeffector activity in an intracellular
811 bacterial pathogen, Legionella pneumophila . *Mol Syst Biol* **12**:893.
812 doi:10.15252/msb.20167381
813 Valleau D, Quaile AT, Cui H, Xu X, Evdokimova E, Chang C, Cuff ME, Urbanus ML,
814 Houliston S, Arrowsmith CH, Ensminger AW, Savchenko A. 2018. Discovery of
815 Ubiquitin Deamidases in the Pathogenic Arsenal of Legionella pneumophila. *Cell Rep*
816 **23**:568–583. doi:10.1016/j.celrep.2018.03.060
817 Vormittag S, Hüsler D, Haneburger I, Kroniger T, Anand A, Prantl M, Barisch C, Maaß S,
818 Becher D, Letourneur F, Hilbi H. 2023. Legionella‐ and host‐driven lipid flux at
819 LCV‐ER membrane contact sites promotes vacuole remodeling . *EMBO Rep* **24**.
820 doi:10.15252/embr.202256007

821 Zuckman DM, Hung JB, Roy CR. 1999. Pore-forming activity is not sufficient for Legionella
822 pneumophila phagosome trafficking and intracellular growth. *Mol Microbiol* **32**:990–
823 1001. doi:10.1046/j.1365-2958.1999.01410.x
824

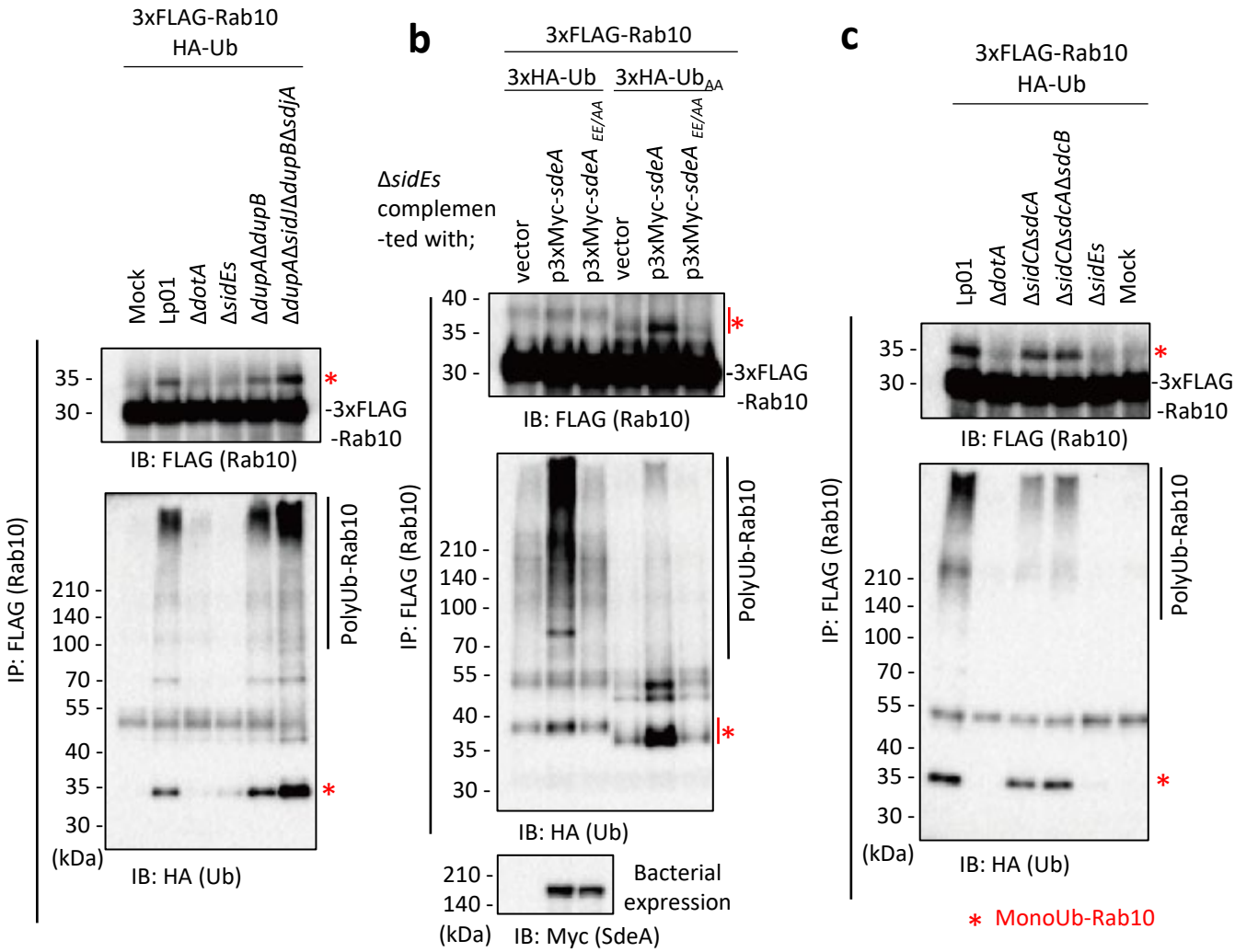
a
3xFLAG-Rab10
HA-Ub
Mock
Lp01
ΔdotA
ΔsidEs
ΔdupAΔdupB
ΔdupAΔsidJΔdupBΔsdjA
35 -
30 -
-3xFLAG
-Rab10
IB: FLAG (Rab10)
IP: FLAG (Rab10)
210 -
140 -
100 -
70 -
55 -
40 -
35 -
30 -
(kDa)
PolyUb-Rab10
IB: HA (Ub)
b
3xFLAG-Rab10
3xHA-Ub
3xHA-Ub$_{\Delta A}$
ΔsidEs
complemen
-ted with;
vector
p3xMyc-sdeA
p3xMyc-sdeA EE/AA
vector
p3xMyc-sdeA
p3xMyc-sdeA EE/AA
40 -
35 -
30 -
-3xFLAG
-Rab10
IB: FLAG (Rab10)
IP: FLAG (Rab10)
210 -
140 -
100 -
70 -
55 -
40 -
35 -
30 -
PolyUb-Rab10
IB: HA (Ub)
210 -
140 -
(kDa)
Bacterial
expression
IB: Myc (SdeA)
c
3xFLAG-Rab10
HA-Ub
Lp01
ΔdotA
ΔsidCΔsdcA
ΔsidCΔsdcAΔsdcB
ΔsidEs
Mock
35 -
30 -
-3xFLAG
-Rab10
IB: FLAG (Rab10)
IP: FLAG (Rab10)
210 -
140 -
100 -
70 -
55 -
40 -
35 -
30 -
(kDa)
PolyUb-Rab10
IB: HA (Ub)
* MonoUb-Rab10

Figure 1

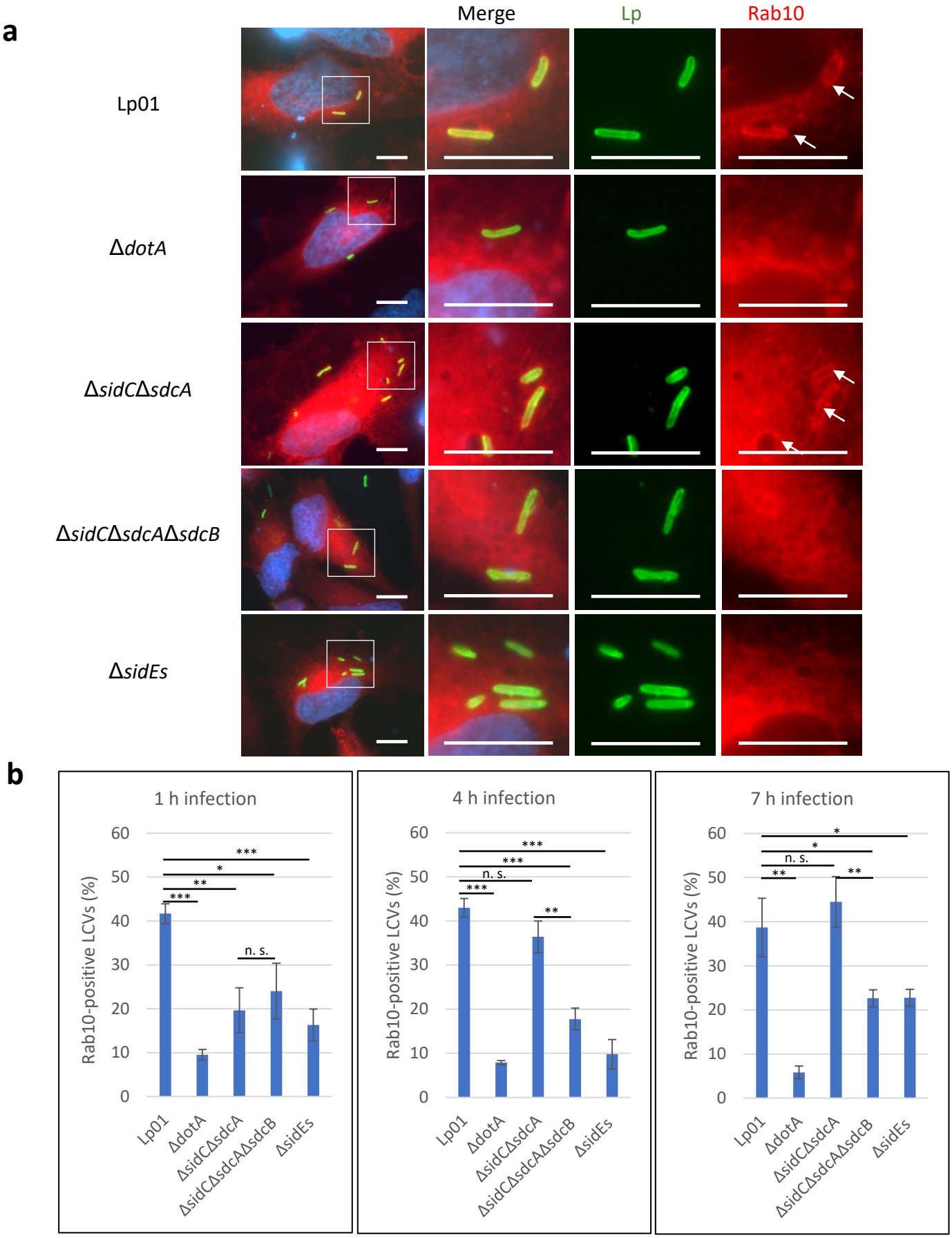
a
Merge
Lp
Rab10
Lp01
ΔdotA
ΔsidCΔsdcA
ΔsidCΔsdcAΔsdcB
ΔsidEs
b
1 h infection
4 h infection
7 h infection
Rab10-positive LCVs (%)
0
10
20
30
40
50
60
***
*
**
n. s.
Lp01
ΔdotA
ΔsidCΔsdcA
ΔsidCΔsdcAΔsdcB
ΔsidEs
* p < 0.02
** p < 0.005
*** p < 0.001

Figure 2

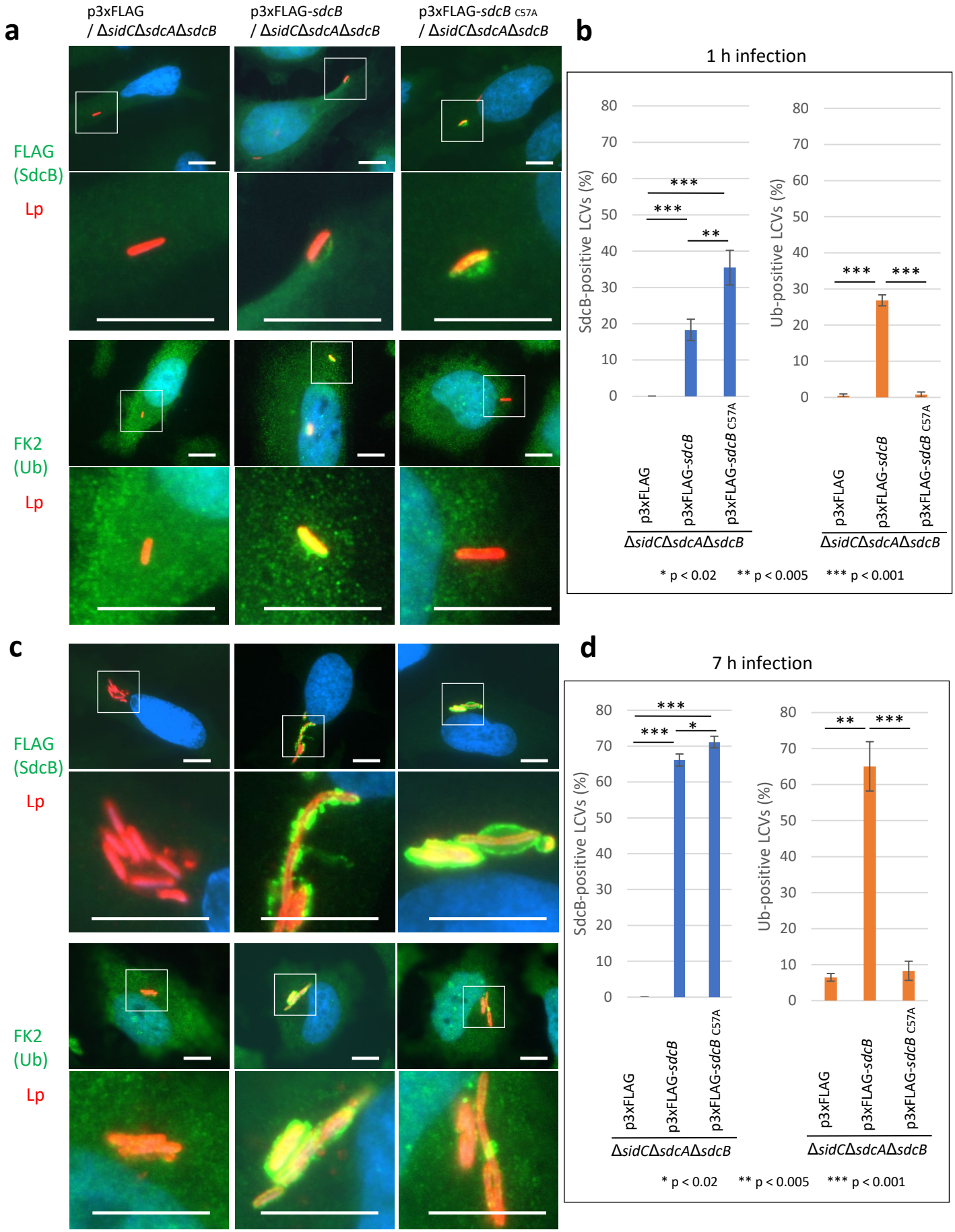
a
p3xFLAG / ΔsidCΔsdcAΔsdcB
p3xFLAG-sdcB / ΔsidCΔsdcAΔsdcB
p3xFLAG-sdcB C57A / ΔsidCΔsdcAΔsdcB
FLAG (SdcB)
Lp
FK2 (Ub)
Lp
b
1 h infection
SdcB-positive LCVs (%)
Ub-positive LCVs (%)
p3xFLAG
p3xFLAG-sdcB
p3xFLAG-sdcB C57A
ΔsidCΔsdcAΔsdcB
* p < 0.02 ** p < 0.005 *** p < 0.001
c
FLAG (SdcB)
Lp
FK2 (Ub)
Lp
d
7 h infection
SdcB-positive LCVs (%)
Ub-positive LCVs (%)
p3xFLAG
p3xFLAG-sdcB
p3xFLAG-sdcB C57A
ΔsidCΔsdcAΔsdcB
* p < 0.02 ** p < 0.005 *** p < 0.001

Figure 3

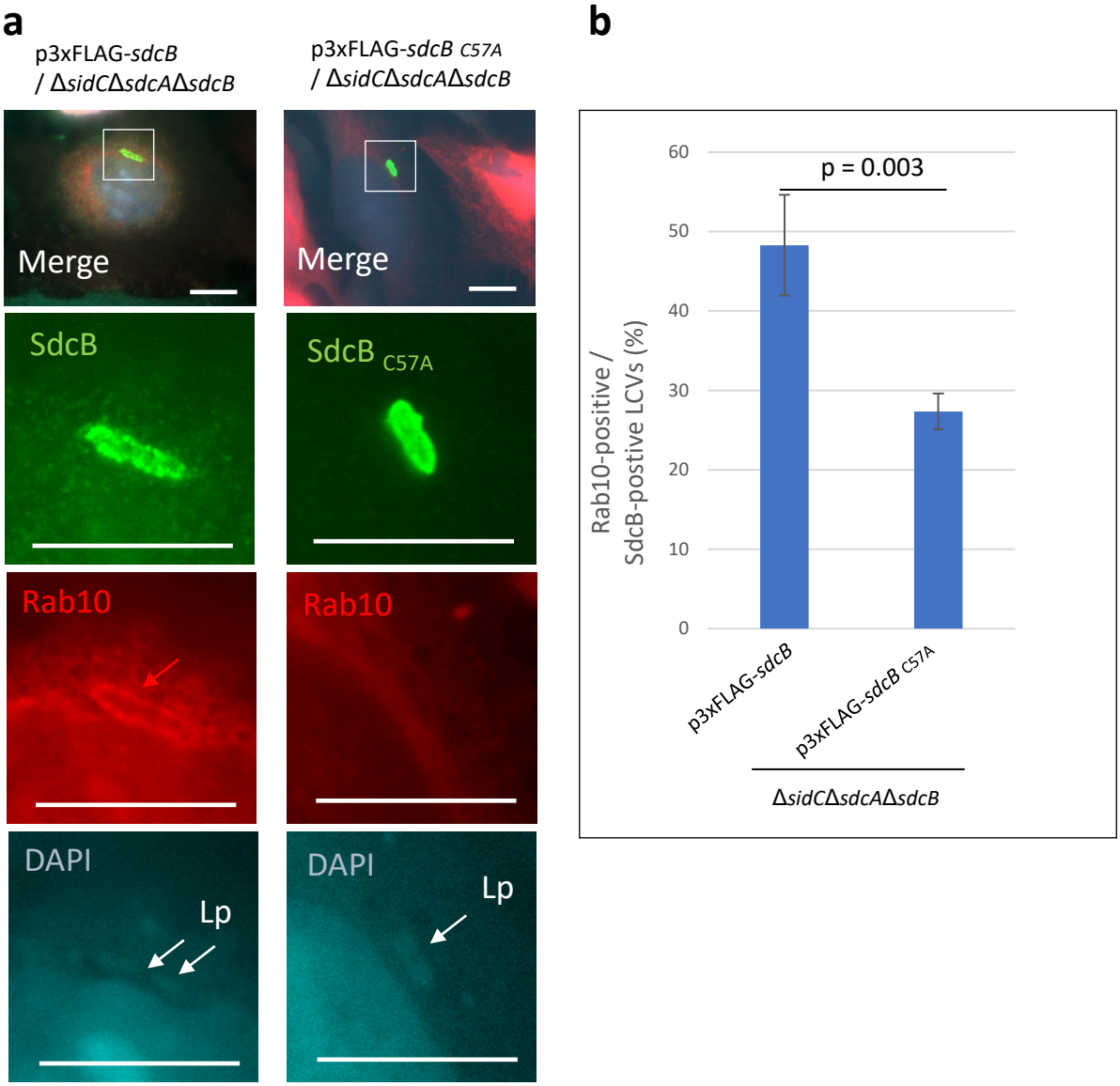
a
p3xFLAG-sdcB / ΔsidCΔsdcAΔsdcB
p3xFLAG-sdcB C57A / ΔsidCΔsdcAΔsdcB
Merge
Merge
SdcB
SdcB C57A
Rab10
Rab10
DAPI
Lp
DAPI
Lp
b
p = 0.003
Rab10-positive / SdcB-postive LCVs (%)
60
50
40
30
20
10
0
p3xFLAG-sdcB
p3xFLAG-sdcB C57A
ΔsidCΔsdcAΔsdcB

Figure 4

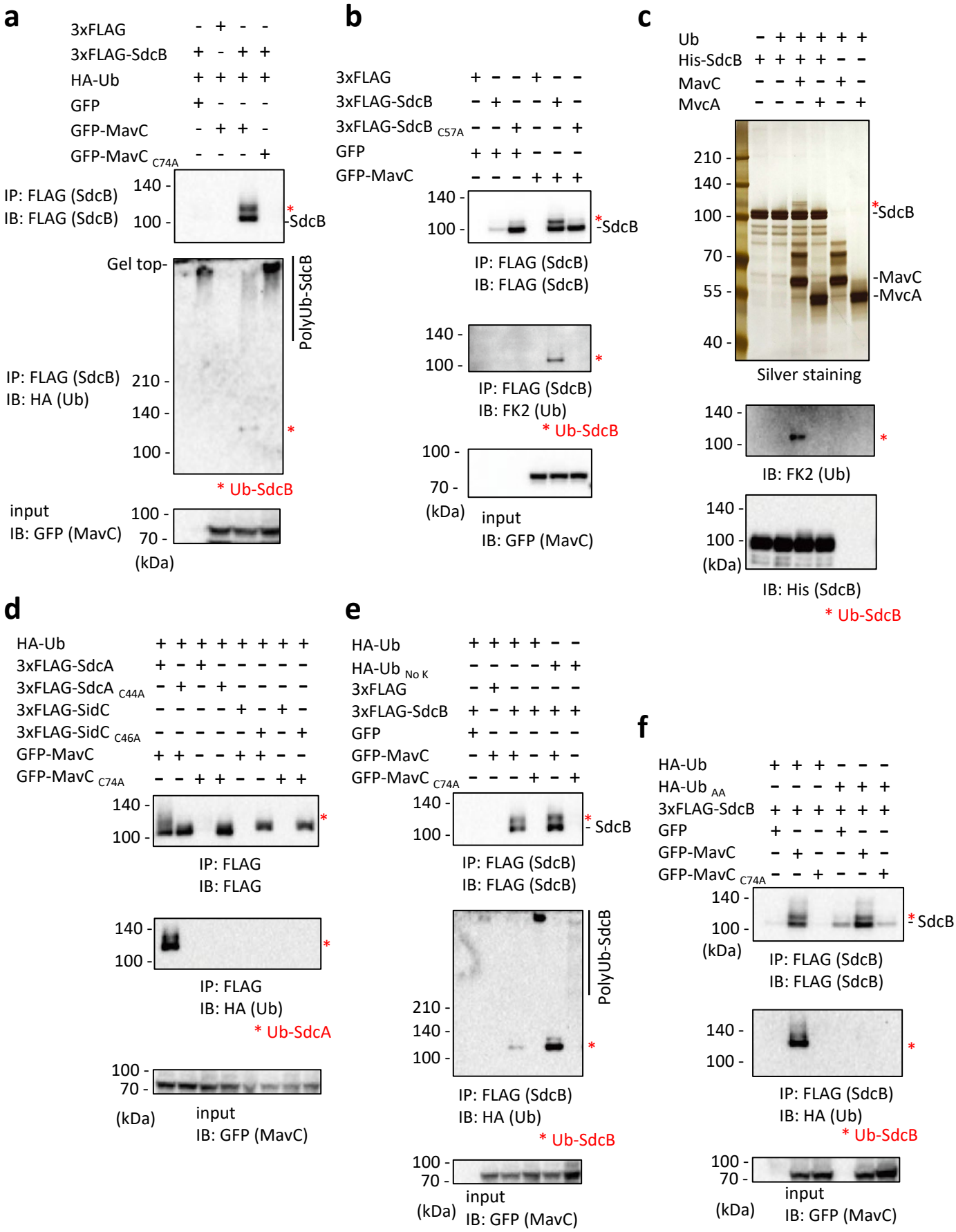
a
3xFLAG - + - -
3xFLAG-SdcB + - + +
HA-Ub + + + +
GFP + - - -
GFP-MavC - + + -
GFP-MavC C74A - - - +
IP: FLAG (SdcB)
IB: FLAG (SdcB)
140 -
100 -
* -SdcB
Gel top-
PolyUb-SdcB
IP: FLAG (SdcB)
IB: HA (Ub)
210 -
140 -
100 -
* Ub-SdcB
input
IB: GFP (MavC)
100 -
70 -
(kDa)
b
3xFLAG + - - + - -
3xFLAG-SdcB - + - - + -
3xFLAG-SdcB C57A - - + - - +
GFP + + + - - -
GFP-MavC - - - + + +
140 -
100 -
* -SdcB
IP: FLAG (SdcB)
IB: FLAG (SdcB)
140 -
100 -
*
IP: FLAG (SdcB)
IB: FK2 (Ub)
* Ub-SdcB
100 -
70 -
(kDa)
input
IB: GFP (MavC)
c
Ub - + + + + +
His-SdcB + + + + - -
MavC - - + - + -
MvcA - - - + - +
210 -
140 -
100 -
70 -
55 -
40 -
*SdcB
-MavC
-MvcA
Silver staining
140 -
100 -
*
IB: FK2 (Ub)
140 -
100 -
(kDa)
IB: His (SdcB)
* Ub-SdcB
d
HA-Ub + + + + + + + +
3xFLAG-SdcA + - + - - - - -
3xFLAG-SdcA C44A - + - + - - - -
3xFLAG-SidC - - - - + - + -
3xFLAG-SidC C46A - - - - - + - +
GFP-MavC + + - - + + - -
GFP-MavC C74A - - + + - - + +
140 -
100 -
*
IP: FLAG
IB: FLAG
140 -
100 -
*
IP: FLAG
IB: HA (Ub)
* Ub-SdcA
100 -
70 -
(kDa)
input
IB: GFP (MavC)
e
HA-Ub + + + + - -
HA-Ub No K - - - - + +
3xFLAG - + - - - -
3xFLAG-SdcB + - + + + +
GFP + - - - - -
GFP-MavC - + + - + -
GFP-MavC C74A - - - + - +
140 -
100 -
* - SdcB
IP: FLAG (SdcB)
IB: FLAG (SdcB)
PolyUb-SdcB
210 -
140 -
100 -
*
IP: FLAG (SdcB)
IB: HA (Ub)
* Ub-SdcB
100 -
70 -
(kDa)
input
IB: GFP (MavC)
f
HA-Ub + + + - - -
HA-Ub AA - - - + + +
3xFLAG-SdcB + + + + + +
GFP + - - + - -
GFP-MavC - + - - + -
GFP-MavC C74A - - + - - +
140 -
100 -
(kDa)
* SdcB
IP: FLAG (SdcB)
IB: FLAG (SdcB)
140 -
100 -
*
IP: FLAG (SdcB)
IB: HA (Ub)
* Ub-SdcB
100 -
70 -
(kDa)
input
IB: GFP (MavC)

Figure 5

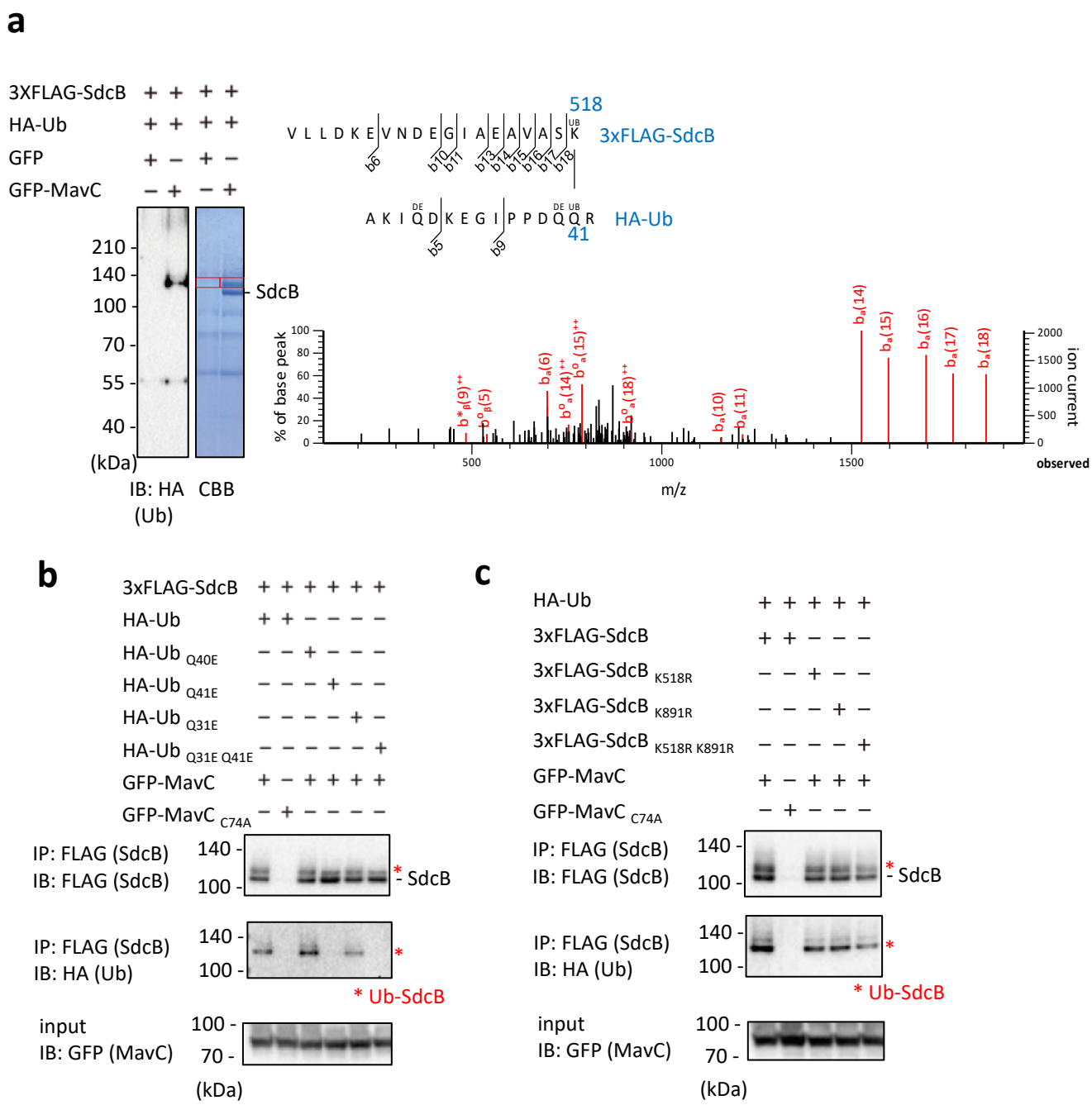
a
3XFLAG-SdcB + + + +
HA-Ub + + + +
GFP + − + −
GFP-MavC − + − +
210
140
100
70
55
40
(kDa)
SdcB
IB: HA (Ub)
CBB
518
V L L D K E V N D E G I A E A V A S K
3xFLAG-SdcB
A K I Q D K E G I P P D Q Q R
HA-Ub
41
% of base peak
m/z
ion current
observed
b
3xFLAG-SdcB + + + + + +
HA-Ub + + − − − −
HA-Ub Q40E − − + − − −
HA-Ub Q41E − − − + − −
HA-Ub Q31E − − − − + −
HA-Ub Q31E Q41E − − − − − +
GFP-MavC + − + + + +
GFP-MavC C74A − + − − − −
IP: FLAG (SdcB)
IB: FLAG (SdcB)
- SdcB
IP: FLAG (SdcB)
IB: HA (Ub)
* Ub-SdcB
input
IB: GFP (MavC)
(kDa)
c
HA-Ub + + + + +
3xFLAG-SdcB + + − − −
3xFLAG-SdcB K518R − − + − −
3xFLAG-SdcB K891R − − − + −
3xFLAG-SdcB K518R K891R − − − − +
GFP-MavC + − + + +
GFP-MavC C74A − + − − −
IP: FLAG (SdcB)
IB: FLAG (SdcB)
- SdcB
IP: FLAG (SdcB)
IB: HA (Ub)
* Ub-SdcB
input
IB: GFP (MavC)
(kDa)

Figure 6

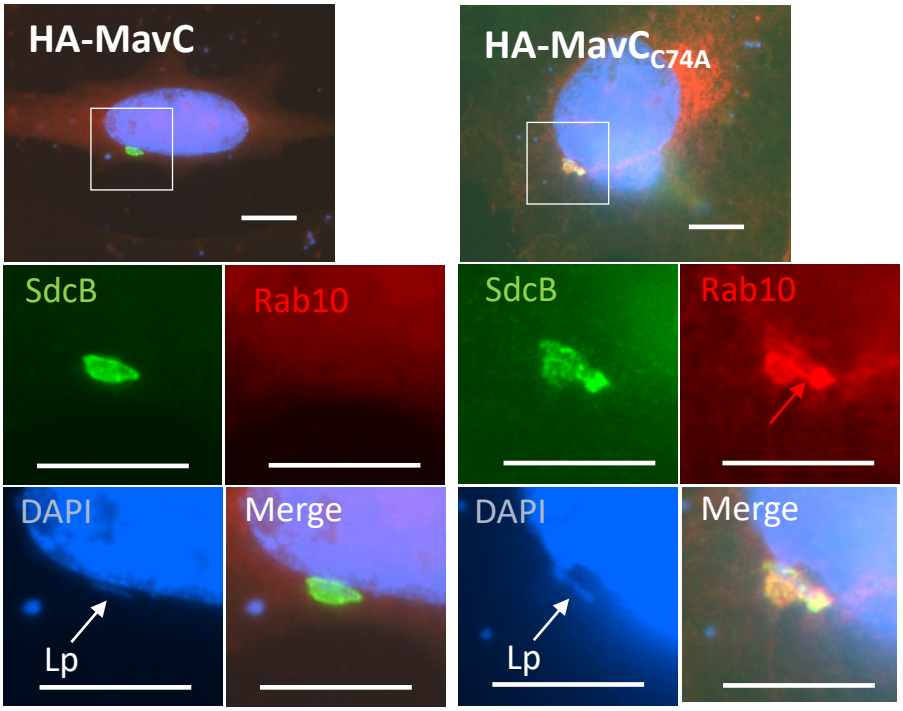
a
HA-MavC
HA-MavC C74A
SdcB
Rab10
SdcB
Rab10
DAPI
Merge
DAPI
Merge
Lp
Lp

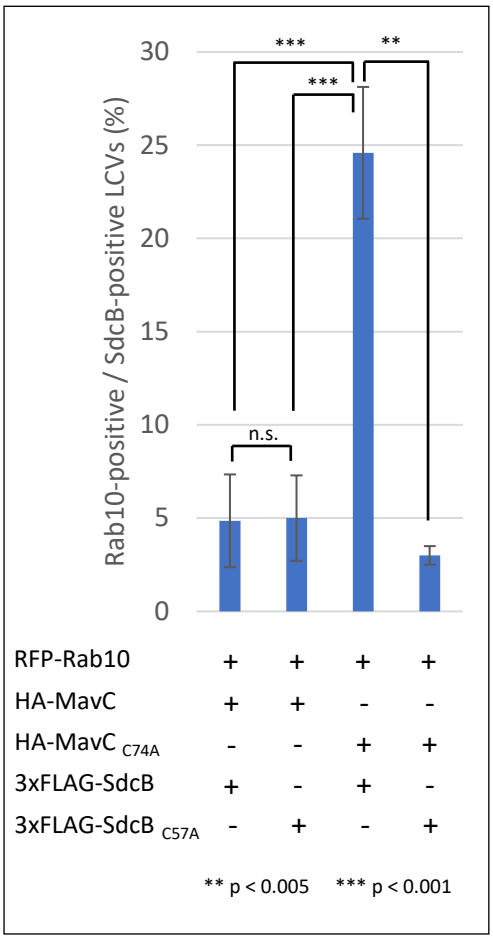
b
Rab10-positive / SdcB-positive LCVs (%)
30
25
20
15
10
5
0
***
***
**
n.s.
RFP-Rab10 + + + +
HA-MavC + + - -
HA-MavC C74A - - + +
3xFLAG-SdcB + - + -
3xFLAG-SdcB C57A - + - +
** p < 0.005
*** p < 0.001

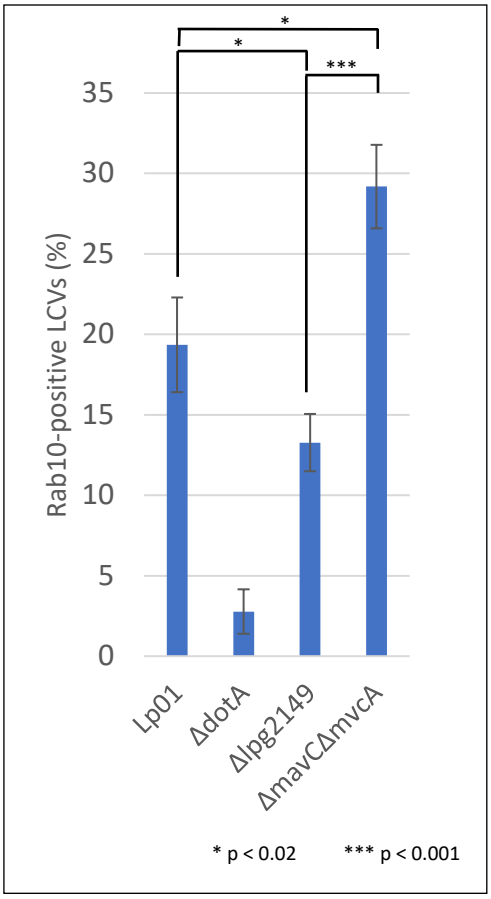
c
Rab10-positive LCVs (%)
35
30
25
20
15
10
5
0
*
*
***
Lp01
ΔdotA
Δlpg2149
ΔmavCΔmvcA
* p < 0.02
*** p < 0.001

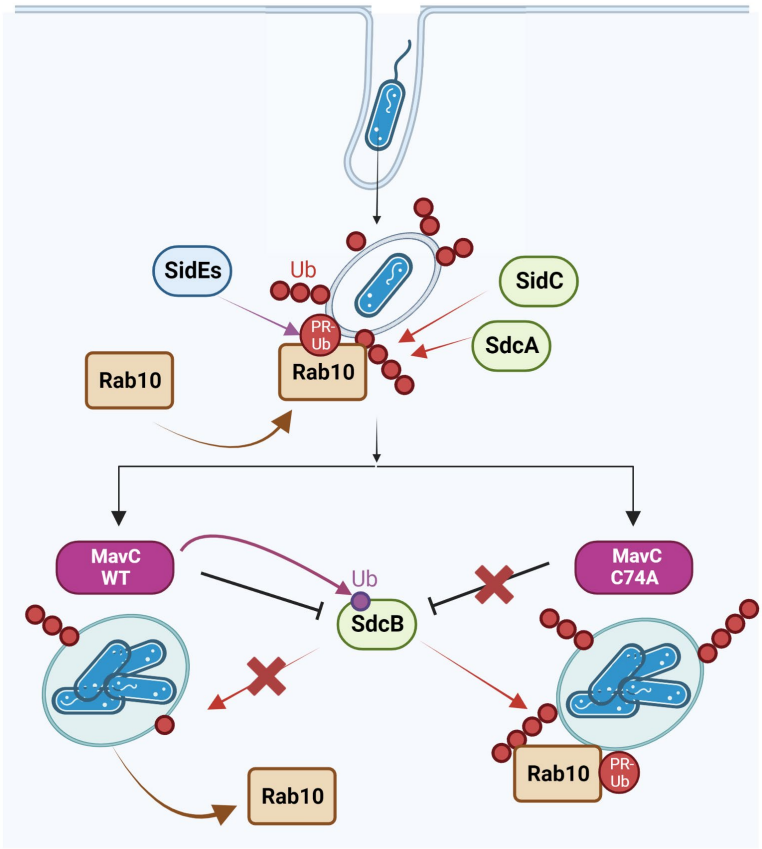
d
SidEs
Ub
SidC
PR-Ub
SdcA
Rab10
Rab10
MavC WT
Ub
SdcB
MavC C74A
Rab10
Rab10
PR-Ub

Figure 7

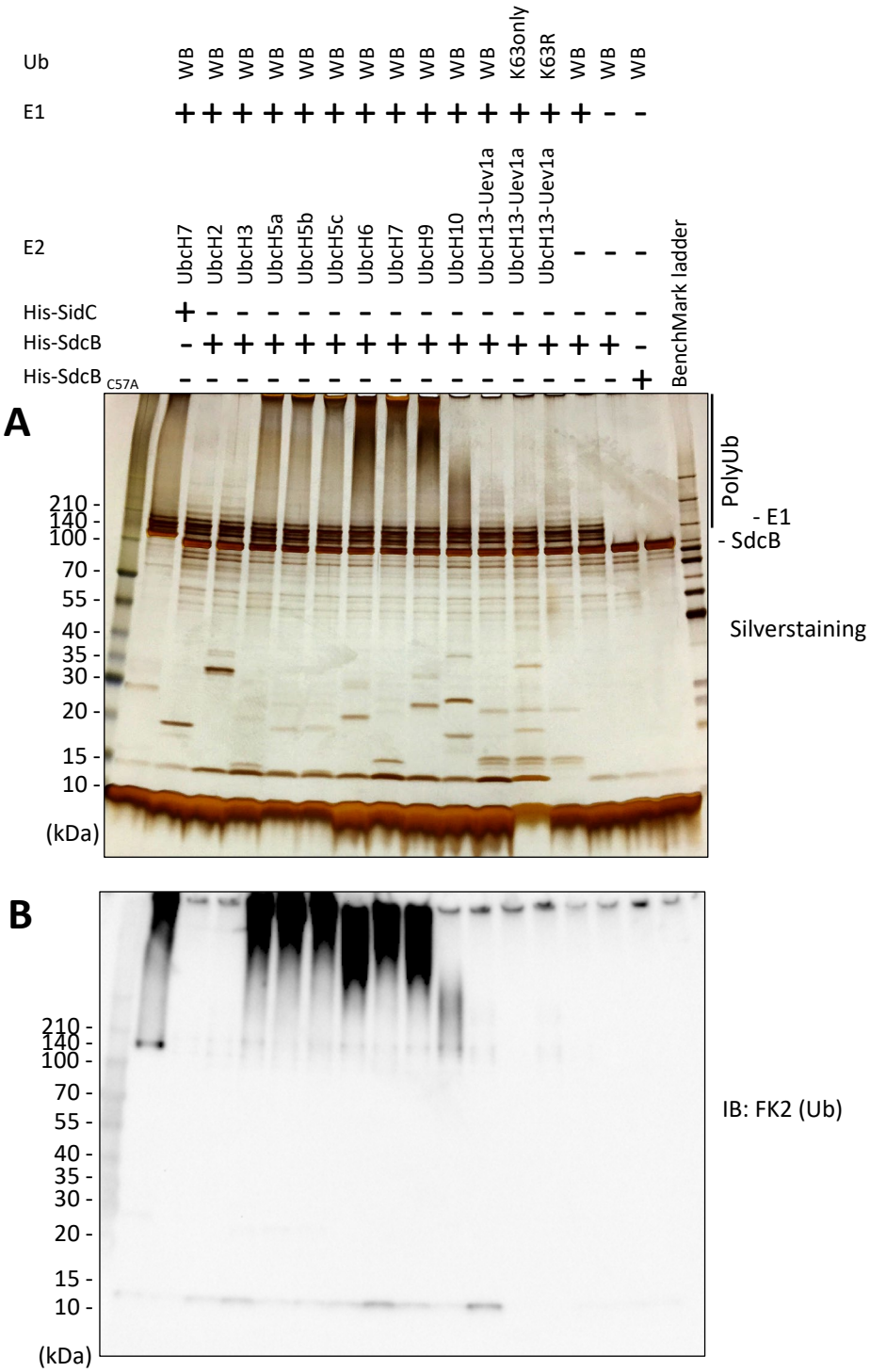

Figure 5 – figure supplement 1

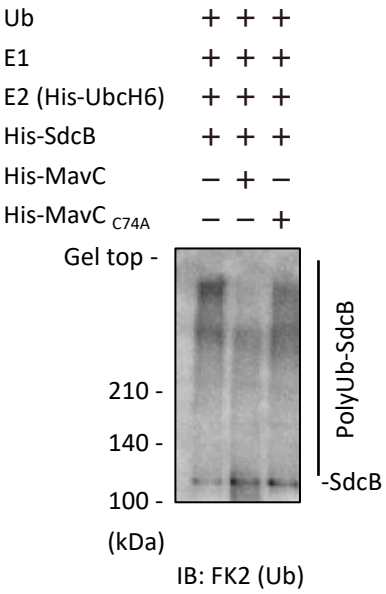

Figure 5 – figure supplement 2

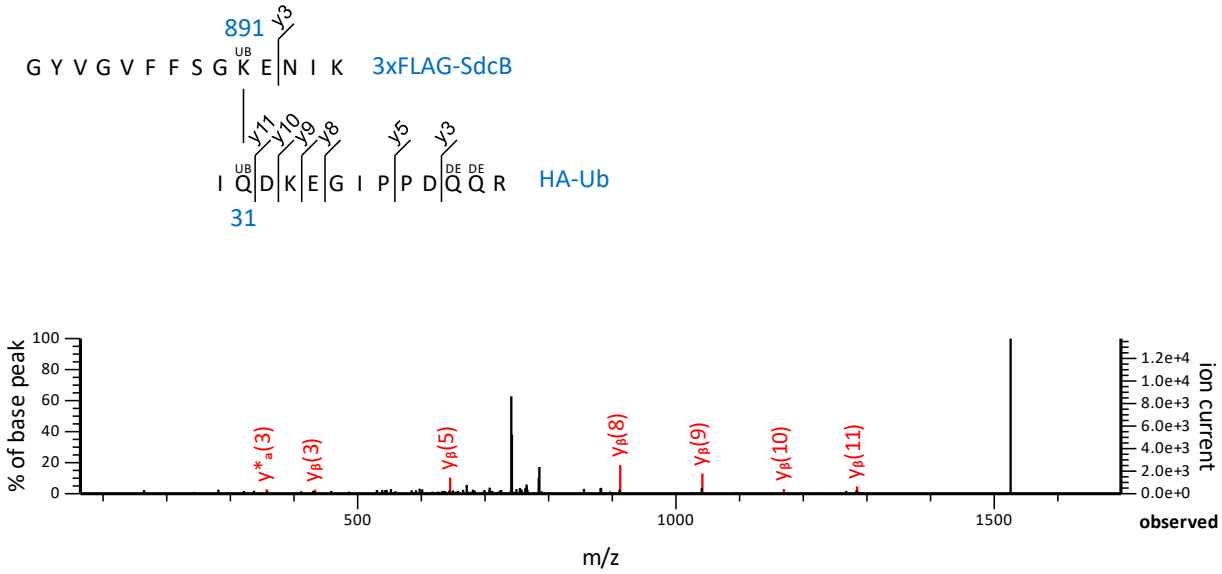

Figure 6 – figure supplement 1

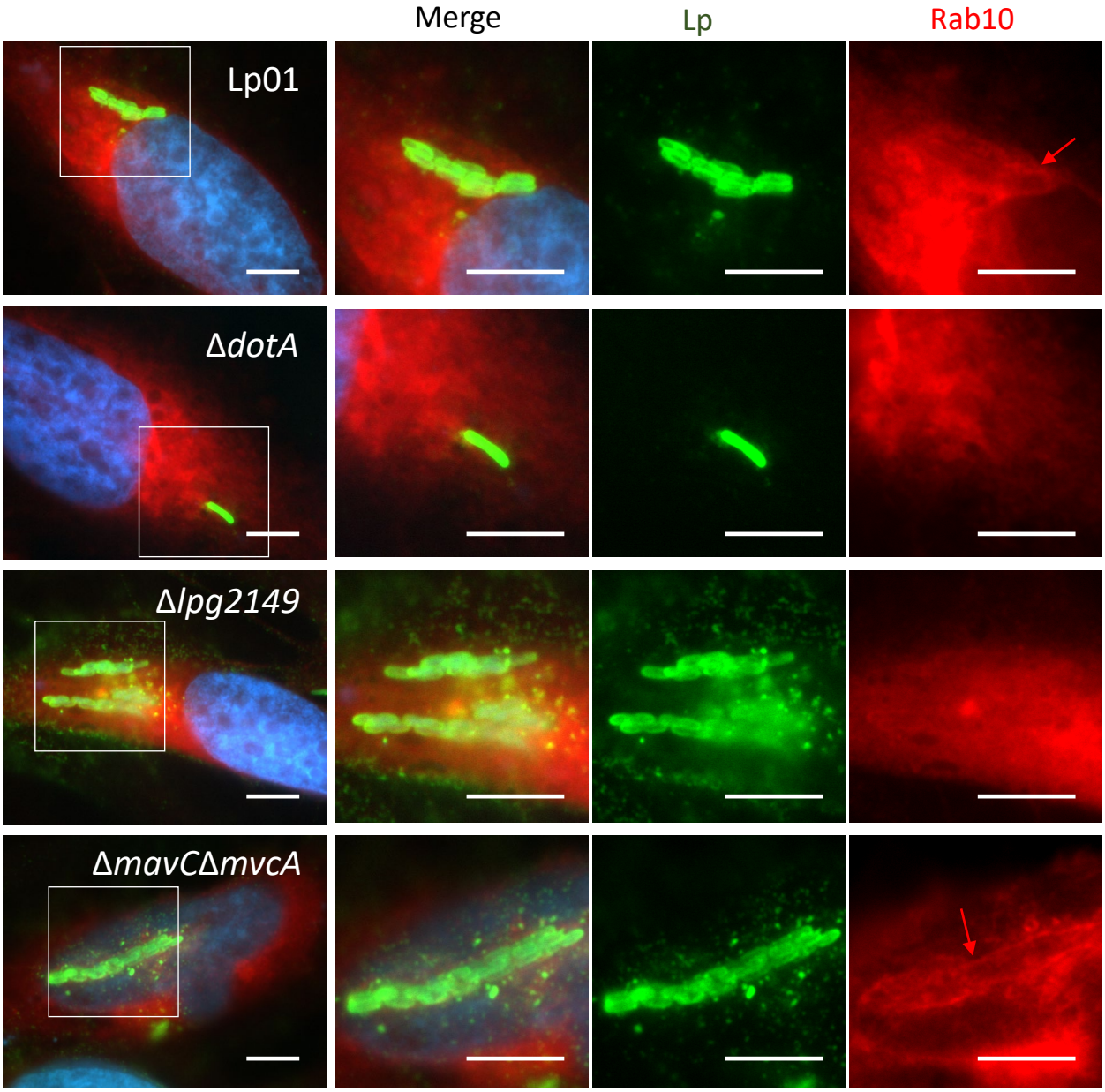

Figure 7 – figure supplement 1

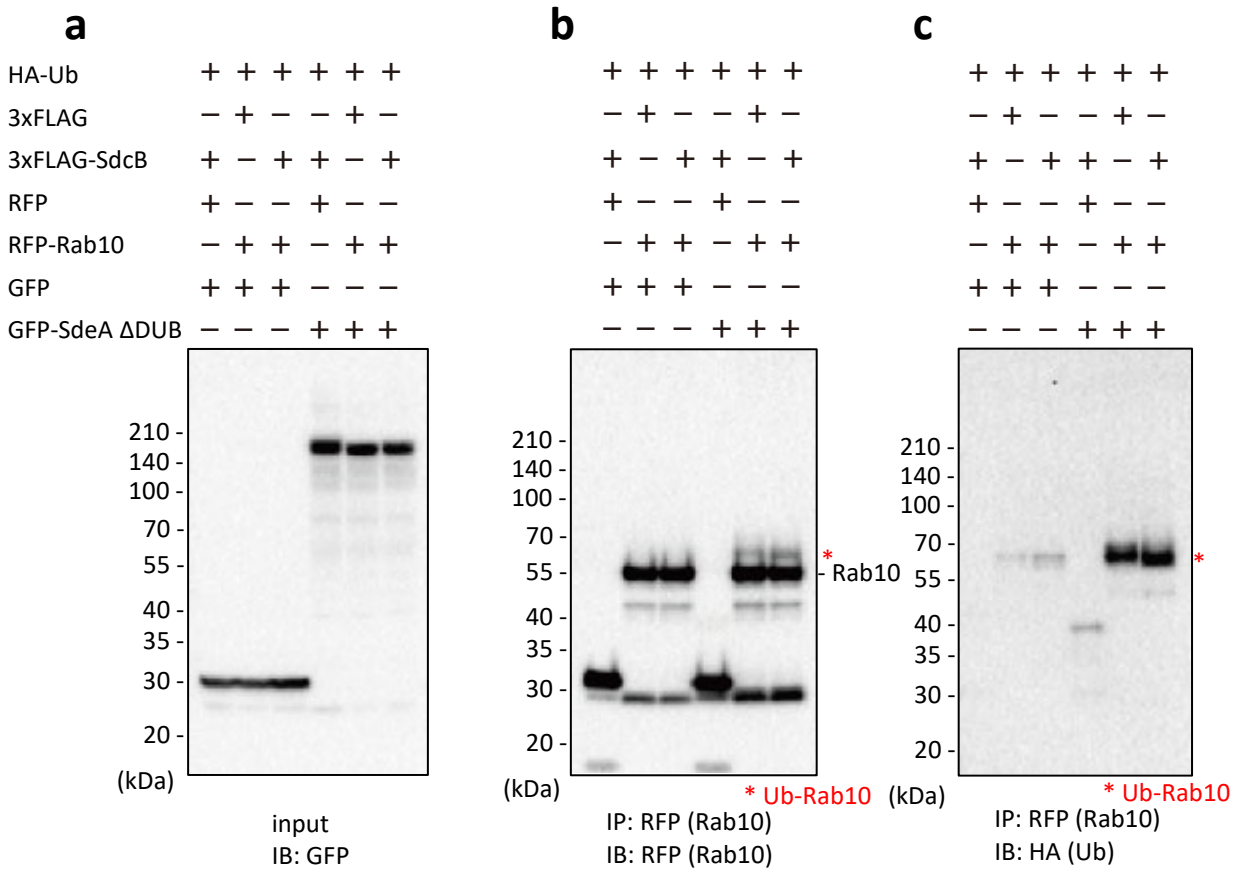

Figure 7 – figure supplement 2